THE NIOBIUM AND TANTALUM CONTENT OF SOME ALKALI IGNEOUS ROCKS

by

DWIGHT G. MOORE, JR.

Submitted in partial fulfillment of the requirements
for the degree of

MASTER OF SCIENCE IN GEOLOGY

NEW MEXICO INSTITUTE OF MINING AND TECHNOLOGY

JUNE 1965

TABLE OF CONTENTS

		Page
LIST OF FIGURES		ii
LIST OF TABLES		iii
ACKNOWLEDGMENTS		v
ABSTRACT		vi
INTRODUCTION		vii
PART I	TRACE ANALYSIS OF ROCKS FOR NIOBIUM AND TANTALUM	1
	Determination of Niobium	5
	Determination of Tantalum	9
	Ion Exchange Separation of Niobium and Tantalum	21
	The Analysis of Niobium and Tantalum	27
	Results and Conclusions	30
PART II	THE NIOBIUM AND TANTALUM CONTENT OF SOME ALKALI IGNEOUS ROCKS	34
	Magnet Cove	37
	Monte Largo	43
	Wet Mountains	47
	Iron Hill	54
	Other Areas	59
	Results and Conclusions	63
APPENDIX I		71
APPENDIX II		82
APPENDIX III		85

LIST OF FIGURES

Figure		Page
1.	Nb_2O_5 Calibration Curve	8
2.	Ta_2O_5 Calibration Curve	12
3.	Absorbance of Ta-Malachite Green Complex vs. Wavelength	14
4.	Effect of Malachite Green Concentration on Extraction	14
5.	Effect of H_2SO_4 Concentration on Extraction	16
6.	Effect of HF Concentration on Extraction	16
7.	Effect of Standing Time Before Extraction	18
8.	Stability of Organic Phase After Extraction	18
9.	Sketch of Ion Exhange Column	22
10.	Elution of Interfering Elements	25
11.	Index Map of Sample Localities	36
12.	Geologic Map of the Magnet Cove Area	39
13.	Geologic Map of Part of the Monte Largo Area	44
14.	Geologic Map of the Wet Mountains Area	48
15.	Geologic Map of the Iron Hill Area	55
16.	Geologic Map of the Gallinas Mountain Area	60

LIST OF TABLES

Table		Page
I	Interfering Elements in the Thiocyanate Determination of Niobium	9
II	Non-Interfering Elements in the Malachite Green Determination of Tantalum	19
III	Interfering Elements in the Malachite Green Determination of Tantalum	20
IV	Elution of Interfering Elements with the 25/20 Acid Solution	26
V	Results of Niobium Analysis	30
VI	Results of Tantalum Analysis	31
VII	Analysis of ML-3 with Added Impurities	32
VIII	Niobium and Tantalum Content of Rocks from the Magnet Cove Area	41
IX	Calculation of the Nb/Ta Ratio of the Magnet Cove Complex	42
X	Niobium and Tantalum Content of Rocks from the Monte Largo Area	45
XI	Niobium and Tantalum Content of Rocks from the Wet Mountains Area	51
XII	Calculation of the Nb/Ta Ratio of the Wet Mountains Complex	53
XIII	Niobium and Tantalum Content of Rocks from the Iron Hill Area	58
XIV	Calculation of the Nb/Ta Ratio of the Iron Hill Complex	59
XV	Niobium and Tantalum Content of Rocks from the Iron Hill Area	62

Table		Page
XVI	Niobium and Tantalum Content of Some Alkali Igneous Rocks	64
XVII	Comparison of Nb/Ta Ratios	65

ACKNOWLEDGMENTS

Special acknowledgment is made to Dr. Dexter H. Reynolds for many helpful suggestions in the laboratory and during the preparation of the manuscript. Also, special acknowledgment is made to Dr. Fredrick J. Kuellmer for his encourgement, aid in the field, and many useful suggestions.

The author is grateful to Dr. Clay T. Smith who willingly gave his time as advisor after the departure of Dr. Kuellmer.

Acknowledgment is made to Dr. Lawrence R. Hathaway for his suggestions and interest in the project.

The author is indebted to R. L. Erickson for supplying samples from the Magnet Cove area and R. L. Parker for aid in obtaining samples from the Wet Mountains area.

The study was financed in part by a grant from the New Mexico Geological Survey and Research Grant (GP 2709) from the National Science Foundation.

In addition, appreciation is extended to my wife, Deborah for assistance in preparing the manuscript.

ABSTRACT

Sensitive and specific spectrophotometric procedures for determining trace amounts of niobium and tantalum in rocks are based on the formation of the Nb-thiocyanate and Ta-malachite green complexes. A preliminary ion exchange separation removes most of the interfering ions. The remaining interferences are volatilized by ashing the exchange resin and treating the residue, with hydrochloric acid and methanol, and then with hot sulfuric acid. By following the outlined procedure, less than 1 ppm. Nb_2O_5 and Ta_2O_5 can be detected in the same 1 gram sample. Replicate analyses of a carbonatite dike sample indicate an average Nb_2O_5 content of 540 ppm. with a standard deviation of 17 ppm. The same sample contains an average of 21 ppm. Ta_2O_5 with a standard deviation of 1 ppm.

The analyses of 52 samples from 6 alkali igneous complexes show that both niobium and tantalum are enriched in alkalic rocks. Also, there is evidence of a relative enrichment of niobium over tantalum in the later forming rocks of a complex. Late carbonatite intrusions contain the highest niobium concentrations and the highest Nb/Ta ratios. Rocks into which carbonatite dikes have been intruded show an appreciable enrichment in niobium at distances of at least 100 feet from the dike contact. This may be a metasomatic or hydrothermal enrichment associated with the late phases of crystallization of a volatile-rich carbonate magma.

THE NIOBIUM AND TANTALUM CONTENT OF SOME ALKALI IGNEOUS ROCKS

INTRODUCTION

The elements niobium and tantalum were discovered in 1801 and 1802, respectively. They remained chemical curiosities for more than 100 years and only recently have they found use in technology. The bulk of the niobium and tantalum produced goes into the manufacture of high-temperature stainless steels. These steels are, in turn, used in the manufacture of jet and rocket engines. In this period of aero-space technology the demand for niobium and tantalum-bearing alloys has increased and, as a result, new potential sources of these metals are being examined.

The enrichment of niobium in alkali igneous complexes has been noted in recent years, but information concerning the tantalum content of alkalic rocks is meager. One reason for the lack of data is the fact that a dependable analytical procedure for trace amounts of tantalum in rocks has not appeared in the literature. In the first part of this thesis analytical procedures for the determination of trace

amounts of both niobium and tantalum are formulated. In the second part, 52 alkali igneous and associated rock samples are analyzed using the newly formulated procedure and the geochemical implications stemming from the analyses are discussed.

PART I

TRACE ANALYSIS OF ROCKS FOR NIOBIUM AND TANTALUM

One of the most difficult tasks of the analytical chemist is the determination of trace amounts of niobium and tantalum in rocks. Two quotations best illustrate the state of the analytical chemistry of these elements prior to 1955. First, Hillebrand and Lundell (1929) stated the following in regard to niobium and tantalum:

"The literature is full of statements which were perhaps more or less true for the particular conditions that led to their formulation, but untrue as generalizations...doubtless many analyses and formulas reported are worthless quantitatively and defective qualitatively." Later, Atkinson, Steigman, Joseph and Hiskey (1952) stated:

"The present unsatisfactory state of analysis may seem particularly surprising as they (niobium and tantalum) were discovered almost a century and a half ago. Two main factors contribute to this situation: the chemical complexity of minerals in which they are found and the colloidal character of aqueous solutions of their compounds, further complicated by the presence of interfering elements from the fourth and sixth transition groups."

In recent years, however, old analytical procedures have been improved and new techniques have been developed.

Neutron activation as well as X-ray spectrography and polarography have been employed in the determination of niobium and tantalum. In addition, successful separations of niobium and tantalum have been made using ion exchange techniques. As a result, it is now possible to do very good niobium and tantalum analysis on material containing more than 0.1% of the pentoxides (Hague and Machlan, 1959; Kallmann et. al., 1962; Furman, 1962). It is also possible to perform a reasonably good trace analysis for niobium (Grimaldi, 1960), but, in spite of recent progress, a good trace method for tantalum in rocks has not appeared in the literature.

At the beginning of this study an investigation was made of the analytical techniques that might be used. According to Meites (1963) the emission spectrograph has a lower limit of detection of 0.001% Nb using the spectral line at 4058.9Å. This sensitivity is adequate for the determination of niobium in most rocks. The lower limit of detection for tantalum is only 0.1% Ta, however, which is far from adequate. Lopez de Azcona (1960) improved the sensitivity somewhat by fluxing tantalum-bearing samples with a mixture of carbon, zinc, and potassium chlorate, but the method still does not have sufficient sensitivity to be useful in most rock analysis.

In an X-ray fluoresence analysis there is an appreciable absorption or enhancement effect caused by the matrix

of the sample. Because of this, it is necessary to isolate the niobium and tantalum or to know the exact composition of the matrix. Mitchell (1957) has proposed a procedure envolving a preliminary chemical separation followed by an arithmetic method of correcting for the matrix effect. The U. S. Bureau of Mines has recently developed an improved X-ray spectrographic procedure which also involves a preliminary chemical separation (personal communication, 1964). Unfortunately, the sensitivity of the X-ray spectrograph is too low for trace analysis since the lower limit of detection is 0.01% of the pentoxides.

Meinke (1959) and Kim and Meinke (1963) have shown that neutron activation analysis offers an extremely sensitive method for the determination of niobium and tantalum. The analysis is based on the formation of the radioactive isotopes Nb^{93} and Ta^{181}. An intense neutron source is required and the lack of suitable equipment prevented trial of this technique.

Kennedy (1961) and Kirby and Freiser (1963) have published procedures for the polarographic analysis of niobium. The sensitivity is low. Without a preliminary concentration the lower limit of detection is only 0.01% Nb_2O_5. A successful polarographic determination of tantalum has not yet been accomplished.

As the present time, spectrophotometric determinations of niobium and tantalum offer the most sensitive and practical means of trace analysis. Sandell (1959) has described the colorimetric determination of niobium and tantalum based on

the formation of their peroxy complexes. Motojima and Hashitani (1961) have reported the determination of niobium with 8-quinolinol. Dinnin (1953) has developed a method for tantalum with pyrogallol. The sensitivity of these methods is not high and the procedures are subject to many interferences.

The most dependable and widely used trace analysis for niobium is based on the formation of the yellow niobium-thiocyanate complex. Recent variations of the niobium-thiocyanate method have been proposed by McDuffie et. al. (1959), Bergstresser (1959), and Grimaldi (1960). Because of its high sensitivity a modification of the procedure described by Grimaldi was used in the determination of niobium.

A sensitive colorimetric tantalum procedure described by Luke (1959) is subject to serious interference from niobium and titanium and is not useful in a rock analysis. Also, a sensitive tantalum-phenylfluorone procedure has been described by Nazarenko in the Russian literature, but the details of the method are not available. The most sensitive of the analytical procedures for tantalum is one described by Kakita and Goto (1962). It is based on the formation of the tantalum-malachite green complex in a hydrofluoric acid-sulfuric acid solution. By modifying the procedure of Kakita and Goto, the sensitivity of the analysis can be extended to less than 0.0001% Ta_2O_5. After a complete study of the tantalum-malachite green spectrophotometric

analysis an analytical procedure was adopted and used in the determination of trace amounts of tantalum in rocks.

Determination of Niobium

The spectrophotometric determination of niobium is based on the procedure described by Grimaldi. The major difference occurs in the process by which the interfering elements are removed. Grimaldi employs a sodium hydroxide fusion to remove the interfering elements, whereas ion exchange separations are used in the modified procedure. The formation of the niobium-thiocyanate complex and the extraction into ethyl acetate are similar. Grimaldi "washes" the organic phase after the extraction to prevent interference from the iron and titanium. This washing step is unnecessary after an ion exchange separation and is omitted.

Reagents and Apparatus

Preparation of high purity Nb_2O_5. Dissolve a 200 mg. sample of high purity Nb_2O_5 in 10 ml. of concentrated hydrofluoric acid. Add 12.5 ml. of hydrochloric acid and 27.5 ml. of water and place the niobium-bearing solution on an ion exchange column prepared and conditioned as described by Hague and Machlan. Wash the column with a solution of 25% hydrochloric acid and 20% hydrofluoric acid according to the procedure of Hague and Machlan. Elute the niobium from the column with a solution of 14% ammonium chloride and 4%

hydrofluoric acid. Precipitate the niobium with cupferron and ignite to the pentoxide at 1100°C.

Standard Nb_2O_5 stock solution. Fuse 100 mg. of pure Nb_2O_5 with 2 grams of potassium pyrosulfate in a covered 50 ml. Pyrex beaker. Dissolve the fusion cake in 15 ml. of hot concentrated sulfuric acid. Cool the resulting solution, transfer to a 100 ml. volumetric flask containing 70 ml. of 18M sulfuric acid, and dilute to the mark with water. The solution contains 1 mg. Nb_2O_5 per ml.

Standard Nb_2O_5 working solution. Dilute the stock solution 1:99 with 18M sulfuric acid to give a solution containing 10 µg. Nb_2O_5 per ml.

Ammonium thiocyanate solution. 25% w./v. in water.

Stannous chloride solution. 40% w./v. in concentrated hydrochloric acid.

Leaching solution. Mix 200 ml. of 25% w./v. tartaric acid with 650 ml. of concentrated hydrochloric acid and dilute to 1200 ml. with water.

Ethyl acetate. Reagent grade.

Spectrophotometer. Baush and Lomb "Spectronic 20".

Preparation of a Calibration Curve

In the preparation of a calibration curve, transfer aliquots of the Nb_2O_5 working solution to 50 ml. borosilicate beakers and fume to dryness. Add one gram of potassium pyrosulfate to each beaker and fuse until a clear melt is

obtained. With a 1 ml. graduated pipet add 0.67 ml. of concentrated sulfuric acid and carefully heat the beaker over a bunsen flame until the fusion cake disintegrates. After cooling, add 20 ml. of leaching solution and heat to clear the solution. Cool the solution and dilute to 25 ml. with water in a volumetric flask. Transfer a 15 ml. aliquot to a 60 ml. separatory funnel, and add 4.5 ml. of water, 5 ml. of ammonium thiocyanate solution and 0.5 ml. of stannous chloride solution and thoroughly mix. Next, add exactly 10 ml. of ethyl acetate. Stopper the separatory funnel and shake vigorously for 1 minute. Determine the absorbance of the organic phase versus a reagent blank at 385 mμ. Figure 1 shows the calibration curve obtained using this procedure. The curve is linear up to 10 μg. of Nb_2O_5.

Discussion

According to Grimaldi the amount of niobium thiocyanate extracted decreases by approximately 1% for a 1°C rise in temperature. This was confirmed and, as a result, a correction is required when the temperature differs by more than 2°C from the temperature at which the calibration curve is prepared. Once the niobium thiocyanate complex is extracted into ethyl acetate it is stable for at least 1 hour.

Table 1 lists the elements that interfere in the thiocyanate determination of niobium. The amount of the interfering element that gives a color equivalent to 1 μg.

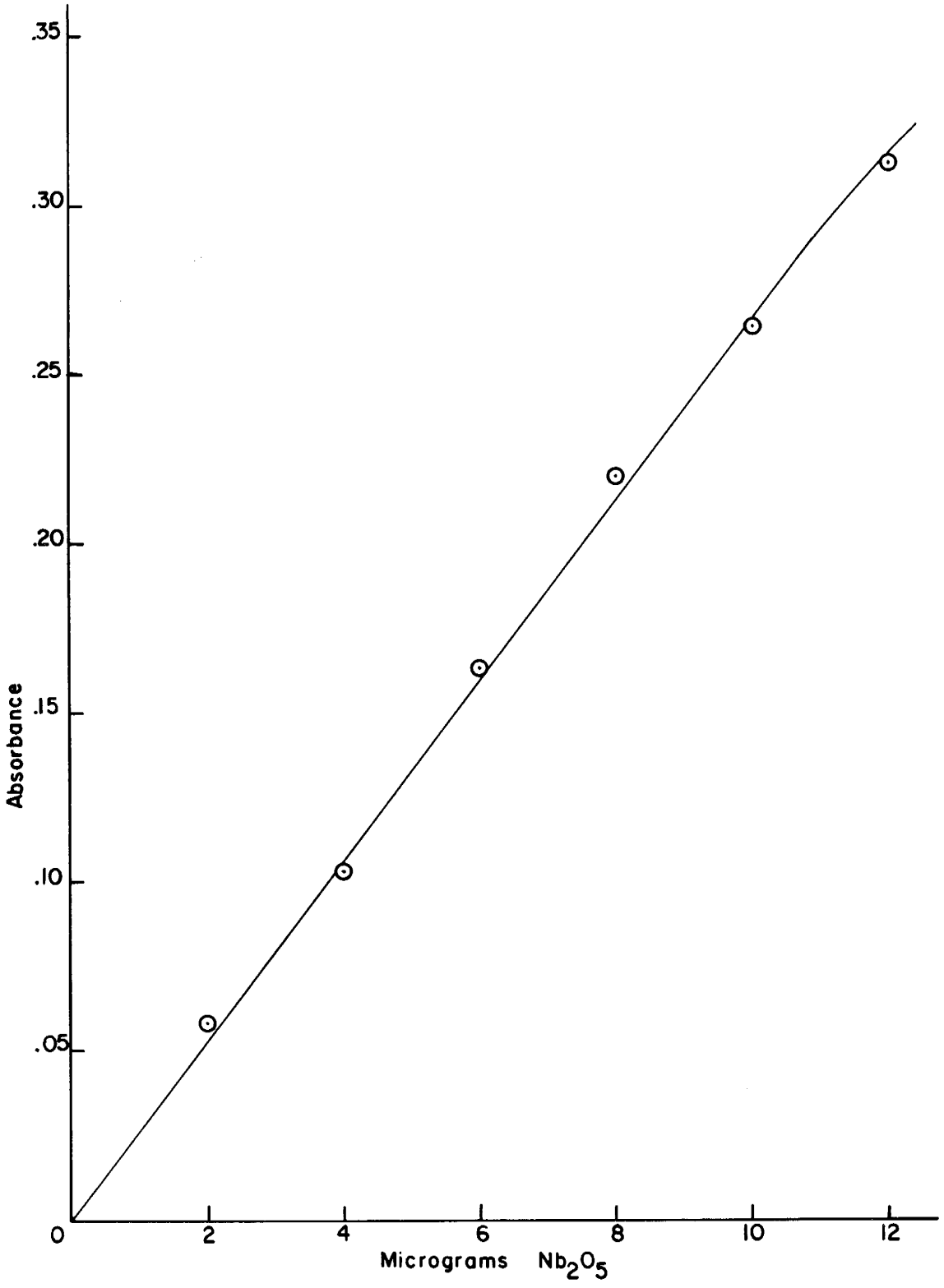

Figure 1. Nb_2O_5 Calibration Curve

of Nb_2O_5 is listed in the second column of the table. In addition to the elements in Table 1, the presence of 10 mg. of titanium, as TiO_2, gives slightly high results and 3 mg. of ZrO_2 gives slightly low results. Of major importance is the fact that 2 mg. of tantalum pentoxide do not interfere.

TABLE I

Interfering Elements in the Thiocyanate Determination of Niobium

Element	Micrograms equivalent to 1 microgram of Nb_2O_5
Re (VII)	4.6
W (VI)	9.5
Pt (IV)	11
V (V)	28
Mo (VI)	60
Cu (II)	880
Au (III)	1100
U (VI)	11,700

Determination of Tantalum

The determination of tantalum is based on the formation of the tantalum-malachite green complex. Because poor reproducibility was experienced in following the procedure of Kakita and Goto, a complete investigation of the analysis was undertaken. Three points were of particular importance:

1. microgram quantities of tantalum tend to hydrolyze in the sulfuric acid-ammonium oxalate solution recommended by Kakita and Goto; 2. the tantalum-malachite green complex is not stable and timing is an important factor in the analysis; 3. serious interference from boron rules out the use of borosilicate glassware in the determination.

In this work the tantalum is placed in solution and kept in solution with hydrofluoric acid. The use of Teflon and polypropylene labware in place of glassware is very satisfactory, but polyethylene becomes contaminated after repeated use.

Reagents and Apparatus

High purity Ta_2O_5. Dissolve a 200 mg. sample of Ta_2O_5 in concentrated hydrofluoric acid. Add sufficient hydrochloric acid and water to give a solution containing 25% hydrochloric acid and 20% hydrofluoric acid by volume. Transfer the solution to an ion exchange column and wash the column with 25/20 acid solution according to the procedure of Hague and Machlan. Next, wash the column with a solution of 14% ammonium chloride and 4% hydrofluoric acid to remove the niobium. Elute the tantalum from the column with a solution of 14% ammonium chloride and 4% ammonium fluoride. Prepare the pure pentoxide by precipitating the tantalum with cupferron and igniting the precipitate at 1100°C.

Ta_2O_5 stock solution. Dissolve 100 mg. of pure Ta_2O_5 in 53 ml. of concentrated hydrofluoric acid in a covered Teflon beaker. Transfer the solution to a 1 liter polypropylene graduated cylinder and dilute to 1 liter with water. Mix the solution and store in a polypropylene bottle. The stock solution contains 100 µg. Ta_2O_5 per ml. in 1.5N hydrofluoric acid and is stable for at least 1 month.

Ta_2O_5 working solutions. Prepare standard solutions containing between 1 and 10 µg. Ta_2O_5 per 2 ml. by appropriate dilutions of the stock solution with 1.5N hydrofluoric acid.

1.5N hydrofluoric acid solution. Dilute 53 ml. of concentrated hydrofluoric acid to 1 liter with distilled water.

Malachite green solution. 0.1% w./v. in water.

Sulfuric acid-ammonium oxalate solution. Dilute 50 ml. of 1N sulfuric acid and 20 ml. of 2% w./v. ammonium oxalate to 250 ml. with water.

Benzene. Reagent grade.

Spectrophotometer. Baush and Lomb "Spectronic 20".

Preparation of a Calibration Curve

Prepare a calibration curve by adding 2 ml. aliquots of the various working standards to 50 ml. polypropylene centrifuge tubes. To each, add 5 ml. of the sulfuric acid-ammonium oxalate solution followed by 3 ml. of malachite green solution. Mix the solution, add exactly 5 ml. of benzene

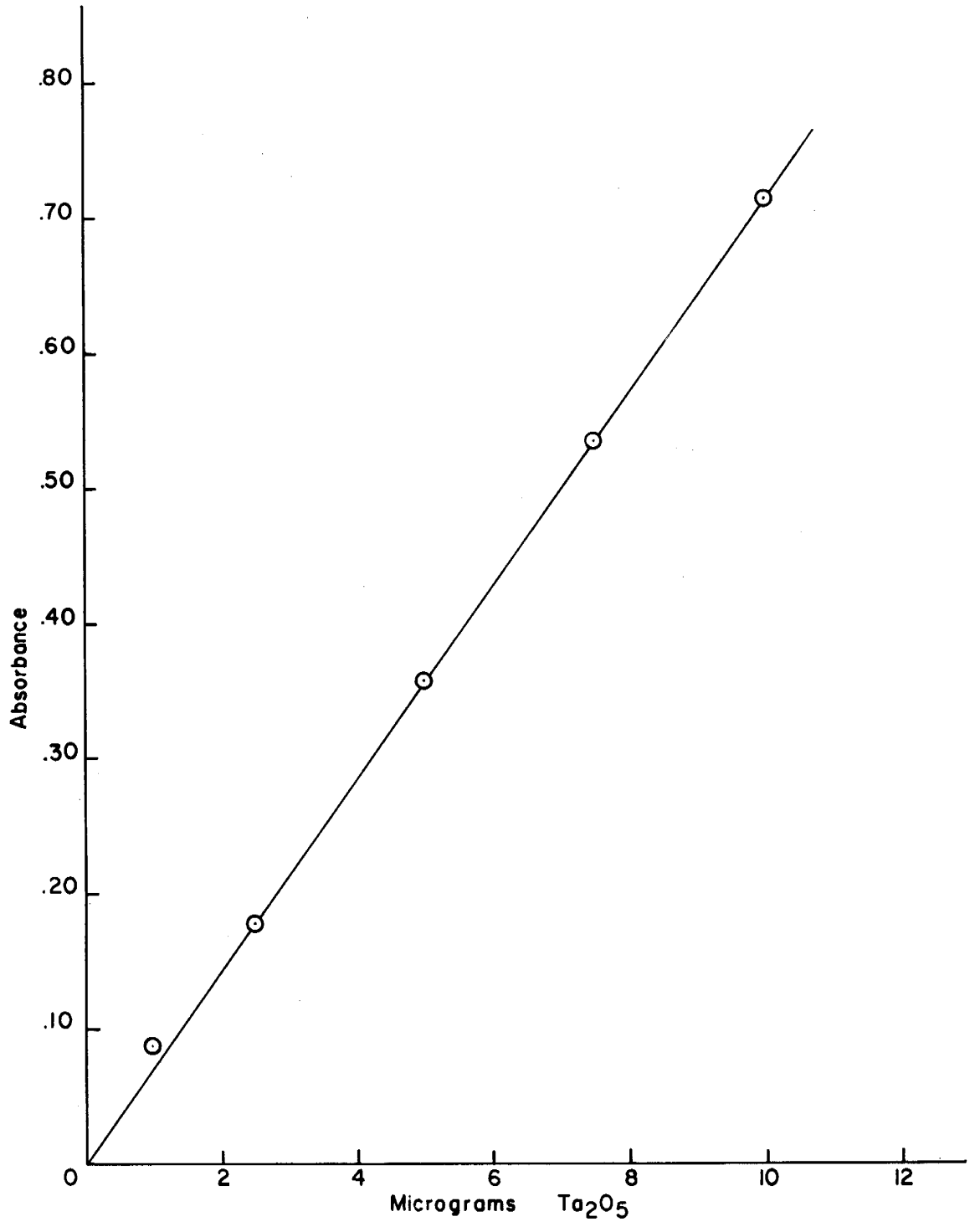

Figure 2. Ta_2O_5 Calibration Curve

and seal the tube. Exactly 2 minutes after the addition of the malachite green shake the tube vigorously for 30 seconds and centrifuge. Exactly 5 minutes after the addition of the malachite green measure the absorbance against benzene at 635 mμ. Subtract the absorbance of a reagent blank to obtain the corrected abosrbance. Figure 2 shows the calibration curve obtained following the above procedure. The curve is linear up to 10 μg. of Ta_2O_5.

Discussion

Figure 3 is a plot of wavelength versus the absorbance of the tantalum-malachite green complex in benzene. The maximum absorbance of the blue complex occurs at 635 mμ.

The effect of varying the malachite green concentration is shown in Figure 4. A volume of 3 ml. of 0.1% malachite green solution gives the maximum corrected absorbance and a fairly low blank value. The graph was obtained by using 5 μg. of Ta_2O_5 and by maintaining all of the variables constant with the exception of the malachite green concentration.

The effect of the sulfuric acid concentration on the extraction is shown in Figure 5. Only the sulfuric acid concentration was varied in obtaining the data. It can be seen from the graph that a maximum extraction occurs when the sulfuric acid concentration of the aqueous phase is 0.1N. An excess of sulfuric acid causes a slight decrease in the absorbance. When the concentration is low there is a sharp decrease in the absorbance.

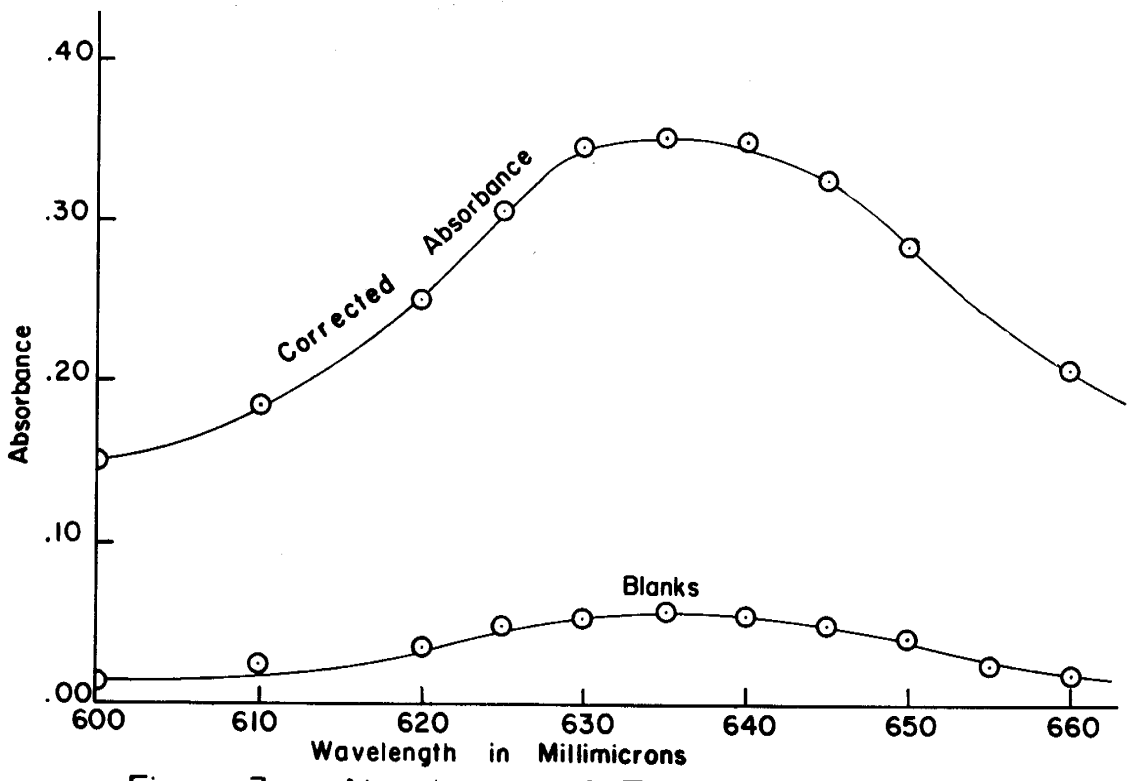

Figure 3. Absorbance of Ta-Malachite Green Complex vs. Wavelength

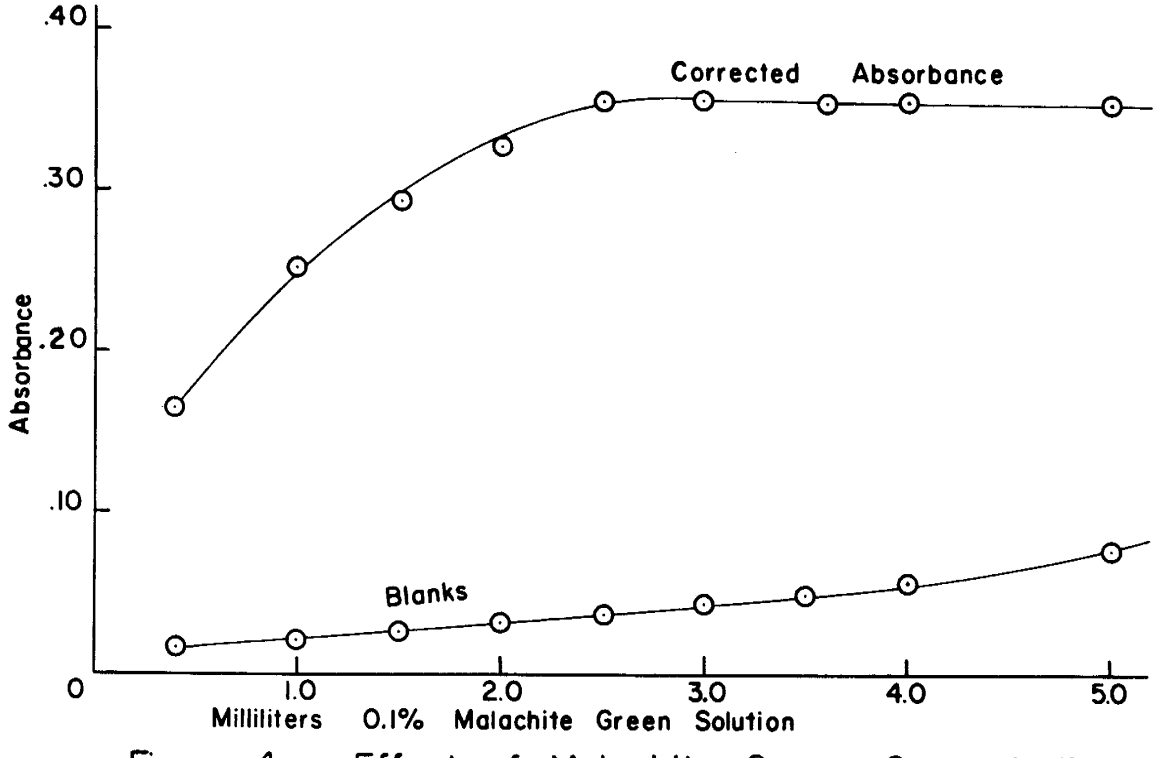

Figure 4. Effect of Malachite Green Concentration on Extraction

The effect of the hydrofluoric acid concentration on the extraction was also determined by maintaining the other variables at constant values. Figure 6 shows the optimum hydrofluoric acid concentration to be 0.3N. An excess of hydrofluoric acid gives high blanks resulting in a decrease in the corrected absorbance of the sample.

The data presented in Figures 3 through 6 confirm the findings of Kakita and Goto. In review, the optimum conditions for extraction are: 1. 3 ml. of 0.1% malachite green solution in a total volume of 10 ml.; 2. a sulfuric acid concentration of 0.1N; 3. a hydrofluoric acid concentration of 0.3N. In addition, ammonium oxalate is added to the aqueous phase as a complexing agent to decrease interfering effects from elements such as tungsten and niobium. Small variations in the ammonium oxalate concentration do not affect the extraction of the tantalum-malachite green complex.

Under the proper conditions, the tantalum-malachite green complex is extremely soluble in benzene. More than 99% of the tantalum is extracted from the aqueous phase with a single 30 second mixing. After the extraction, centrifuging is necessary to give a clean and rapid separation of the two phases. High values of absorbance are obtained when droplets of the aqueous phase are present in the benzene.

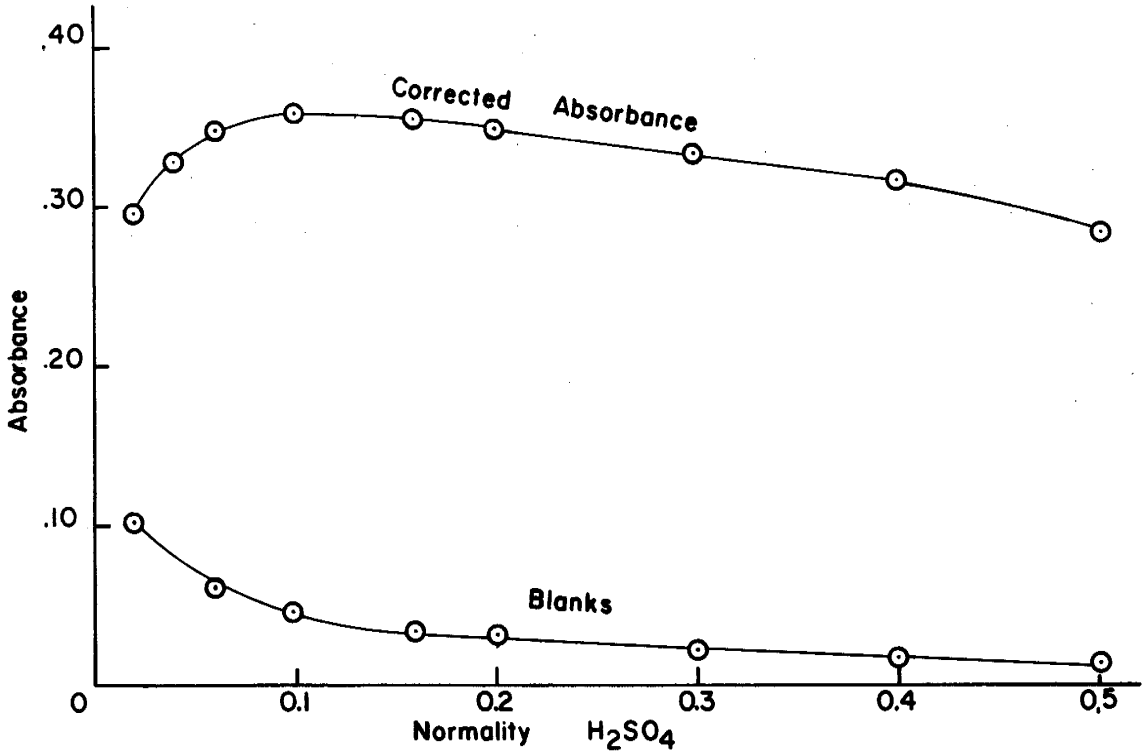

Figure 5. Effect of H_2SO_4 Concentration on Extraction

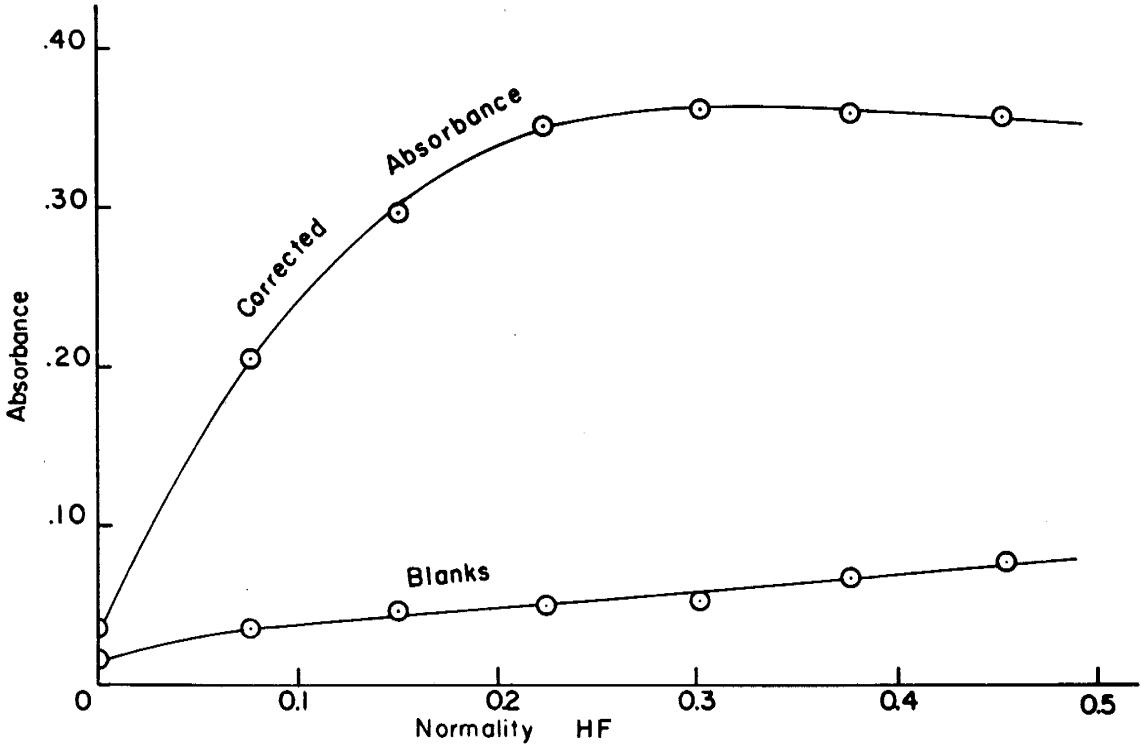

Figure 6. Effect of HF Concentration on Extraction

The absorbance of the tantalum-malachite green complex decreases with time, therefore, careful timing is vital in obtaining consistent results. A 30 minute interval between the addition of the malachite green and the extraction results in a decrease in the color intensity by a factor of approximately one third. The effect of the time lapse between the addition of the dye and the extraction of tantalum is shown in Figure 7. After the tantalum-malachite green complex is extracted into benzene the intensity of the color decreases with time as shown in Figure 8. The color is very sensitive to "dirty" spectrophotometer cells and traces of contamination result in a rapid increase in the absorbance of the blank and samples. Although the colored complex is unstable, with careful timing and clean spectrophotometer cells it is possible to obtain good reproducibility in the analysis of tantalum-bearing samples.

Interfering Elements

Out of a total of 50 elements tested, 16 form analogous blue complexes with malachite green. Table II lists the elements that do not interfere in amounts up to 1 mg. It is significant that niobium is included in Table II. Table III lists the interfering elements. Although Cr (VI) is a major interference it should be noted that Cr (III), the common oxidation state in rocks, does not interfere. Antimony is an interference only in the presence of chloride. In the absence of chloride, 500 µg. of antimony do not interfere.

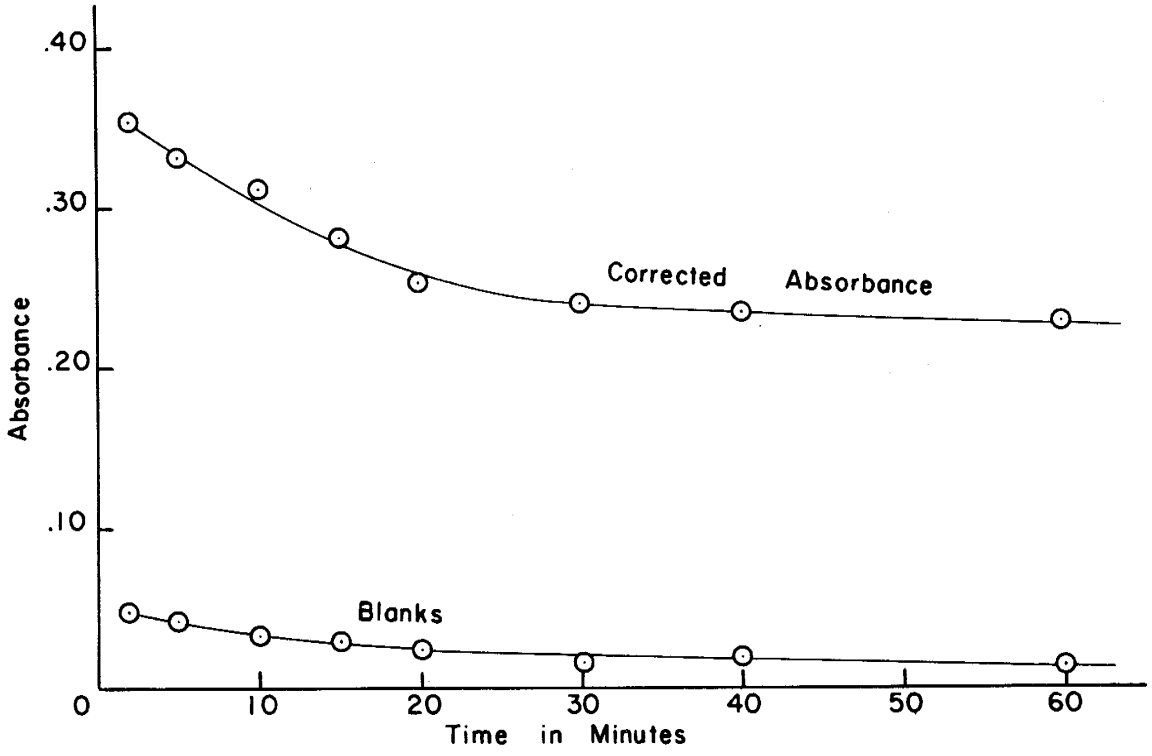

Figure 7. Effect of Standing Time Before Extraction

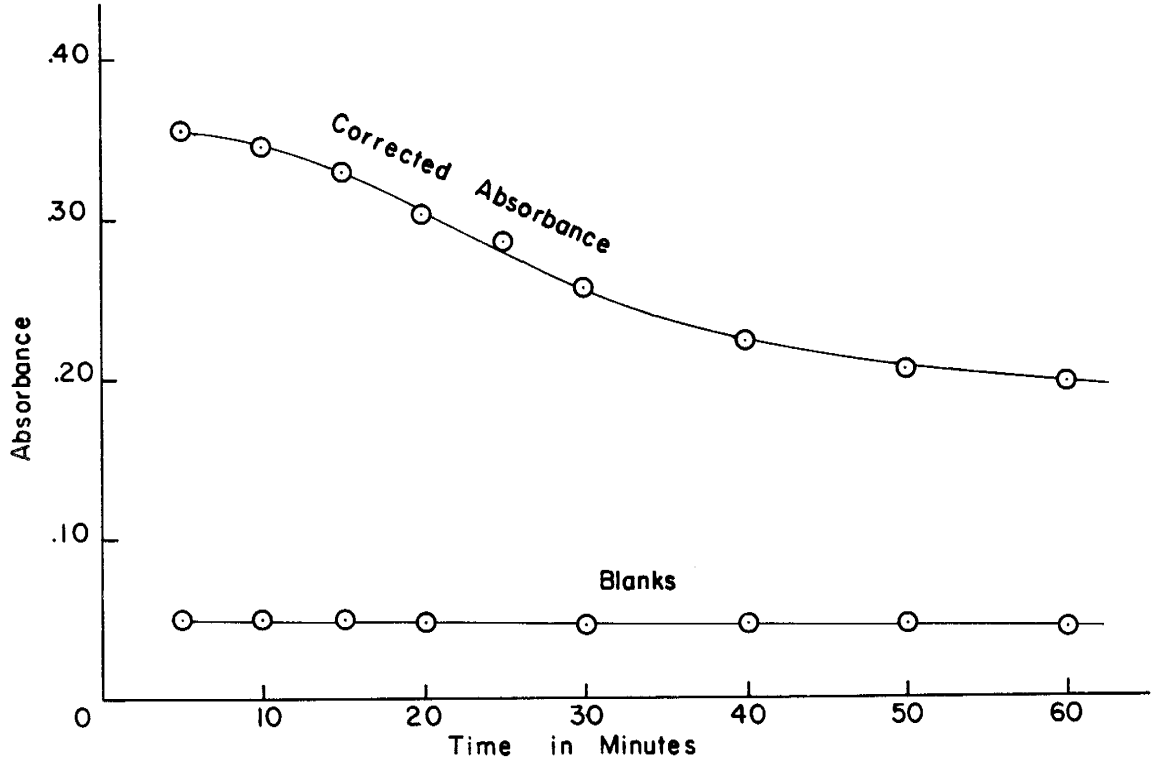

Figure 8. Stability of Organic Phase After Extraction

In addition, nitrate, perchlorate, and iodide react with malachite green to give blue complexes. The fumes from an opened bottle of nitric acid in the vicinity during the color formation are sufficient to cause serious error in an analysis.

TABLE II.

Non Interfering Elements in the Malachite Green Determination of Tantalum*

Group	Element
Ia	Li, Na, K, Rb, Cs
IIa	Be, Mg, Ca, Sr, Ba
IIb	Y (III)
IVb	Ti (IV)
Vb	Nb (V)
VIb	Cr (III)
VIIb	Mn (II)
VIIIb	Fe (II), Fe (III), Ru (III), Co (II), Ni (II)
Ib	Cu (II), Ag (I)
IIb	Zn (II), Cd (II), Hg (II)
IIIa	Al (III), Ga (III)
IVa	Si (IV), Ge (IV), Pb (II)
Va	As (III), Bi (III)
VIa	Se (IV), Te (IV)
R. E.	U (VI)

* In amounts up to 1 mg.

TABLE III

Interfering Elements in the Malachite Green Determination of Tantalum

Element	Micrograms added	Micrograms Ta_2O_5 added	Micrograms Ta_2O_5 found	Micrograms equivalent to 1 microgram Ta_2O_5
B (III)	10	2.5	5.2	3.7
Re (VII)	10	"	5.0	4.0
Cr (VI)	10	"	3.9	7.2
Sb (III)*	100	"	7.6	20
Sn (IV)	100	"	4.8	43
Mo (VI)	100	"	4.2	59
V (V)	100	"	4.0	66
Th (IV)	100	"	3.4	111
Pt (IV)	100	"	3.2	143
Ce (IV)	100	"	3.0	200
Os (III)	100	"	3.0	200
Pd (IV)	100	"	3.0	200
W (VI)	100	"	2.6	1000
Hf (IV)	1000	"	3.4	1110
Zr (IV)	1000	"	2.9	2500
Cu (II)	1000	"	2.9	2500

* With Cl^- present

Ion Exchange Separation of Niobium and Tantalum

In the previous discussion it was shown that a relatively large number of elements interfere in the colorimetric determination of niobium and tantalum. It is, therefore, necessary to remove these interfering elements. The isolation of niobium and tantalum using ion exchange techniques has been reported by Kraus and Moore (1951) and confirmed by Hague and Machlan (1959), Bandi et. al. (1961), Kallmann et. al. (1962), Huff (1964), and others. In most of the reports, hydrofluoric acid-hydrochloric acid solutions are used to accomplish the separations. Also, the use of oxalic acid-hydrochloric acid solutions are described, but separations in an oxalic acid media are less sharp and require larger volumes of eluent. With the exception of Bergstresser's niobium procedure, ion exchange separations have been confined to a macro scale. It is surprising that there has not been a greater application of ion exchange separations in the trace analysis of niobium and tantalum in rocks.

Apparatus and Resin

Ion exchange columns. The large columns used by Hague and Machlan and Kallmann et. al. are not suitable for isolating and recovering microgram amounts of niobium and tantalum. Figure 9 is a diagram of the smaller column that was developed for the isolation of microgram amounts of niobium and tantalum.

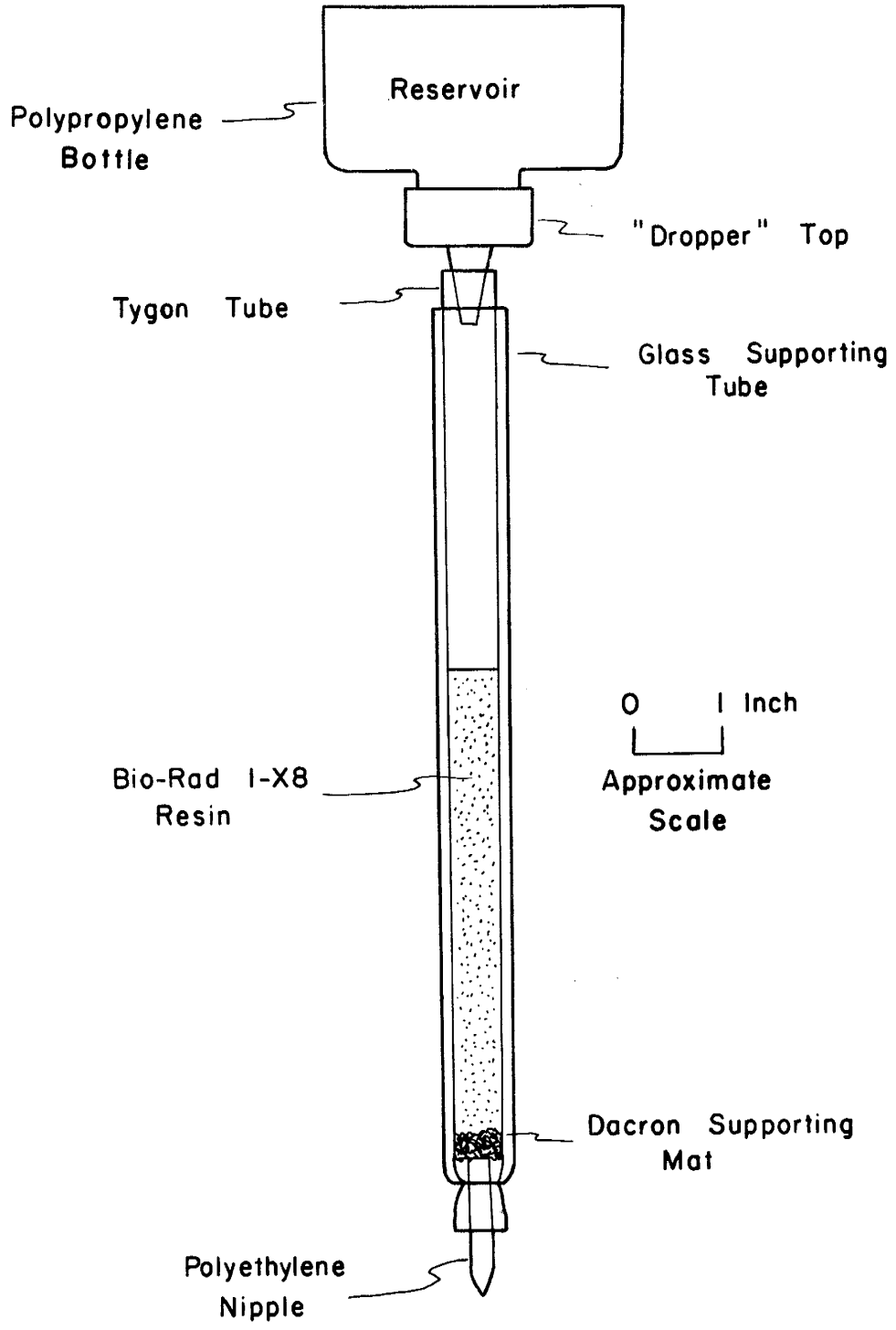

Figure 9. Sketch of Ion Exchange Column

The reservoir consists of half of a 100 ml. polypropylene bottle fitted with a dropper top. The dropper is inserted into a 12" length of 3/8" Tygon tubing. The Tygon tubing is supported by a piece of 1/2" Pyrex tubing which has a slight constriction at the lower end. A nipple made from 1/4" polyethylene tubing is inserted into the lower end of the Tygon tubing. A thin mat of Dacron fibers is supported by the nipple. The Dacron, in turn, supports the resin column. A thin film of stopcock grease on the reservoir dropper insures against the formation of air pockets in the column. With repeated use the Tygon tubing becomes opaque, but this apparently has no ill effect on the analysis.

Resin. AG 1-X8 resin, 100-200 mesh, processed from Dowex 1-X8 resin by Bio-Rad Laboratories was used for the separations. It is a high purity, strongly basic anion exchange resin composed of quarternary ammonium exchange groups attached to a styrene-divinylbenzene polymer lattice.

Dry the resin at room temperature for 72 hours. Add 2.5 grams of resin to the column and wash the column with 20 ml. of 4N hydrochloric acid to insure that the resin is in the chloride form. The flow-rate of the column, adjusted by varying the thickness of the Dacron mat, should be between 30 and 40 ml. per hour.

25/20 acid solution. 25% hydrochloric acid and 20% hydrofluoric acid v./v. in water.

Behavior of Interfering Elements on the column

Cations are not held by the anion exchange resin and quickly pass through the column. Since most of the transition elements can exist in solution as negatively charged complexes the column behavior of these elements can not be predicted with certainty. Hague and Machlan and others have shown that in the 25/20 acid solution both niobium and tantalum are tightly held by the 1-X8 resin. The ion exchange behavior of 11 elements interfering in the determination of niobium and tantalum was investigated and the results are shown in Figure 10. The volume of 25/20 wash solution includes 2 ml. used to prime the columns. Table IV lists the elements and the amounts of 25/20 acid solution required for a 99% elution from the column.

The elements were added to the column in 10 ml. of 25/20 acid solution. All of the elements show a considerable amount of "tailing" (see Figure 10), but with the exceptions of boron and antimony all are removed by a reasonable volume (60 ml.) of eluent. Since the boron content of most rocks is small and since most of the boron is washed from the column with 60 ml. of eluent, the carry over is easily removed by volatilization as methyl borate.

Large volumes of eluent remove only small amounts of antimony from the column. The removal of antimony is not necessary, however, since all traces of chloride may be

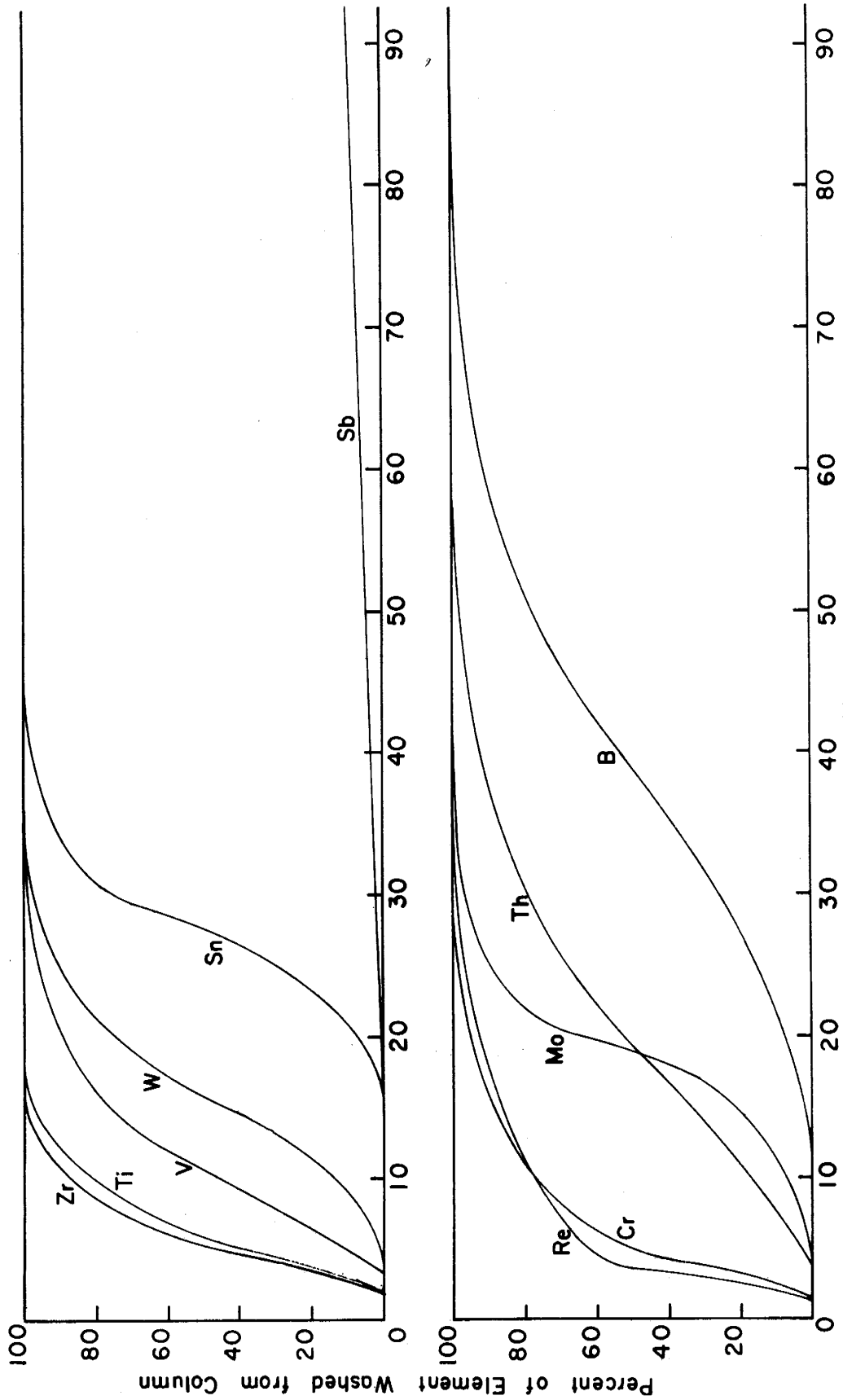

Figure 10. Elution of Interfering Elements

TABLE IV

Elution of Interfering Elements with the 25/20 Acid Solution

Element	Method of Analysis	Reference	Volume required to elute 99%
Zr (IV)	Phenylfluorone	Sandell	20 ml.
Ti (IV)	Peroxide color	Sandell	20 ml.
W (VI)	Thiocyanate color	Sandell	35 ml.
Re (VII)	Malachite green color	Ta-procedure	40 ml.
Mo (VII)	Thiocyanate color	Sandell	45 ml.
V (V)	Peroxide color	Sandell	45 ml.
Sn (IV)	Phenylfluorone color	Sandell	50 ml.
Cr (VI)	Malachite green color	Ta-procedure	50 ml.
Th (IV)	Morin color	Sandell	60 ml.
B (V)	Malachite green color	Ta-procedure	90 ml.
Sb (III)	Malachite green color	improvised	over 100 ml.

removed by fuming the resin ash with sulfuric acid. Platinum and palladium are also held by the resin, but these elements are reduced to the metallic state during the ignition of the resin and do not interfere.

In regard to cerium and the other rare earths, Kallmann et. al. found that the rare earth elements are not retained by the I-X8 resin in an acid solution. If osmium is present it is volatilized by fuming the resin ash with sulfuric acid. Hafnium, being very similar chemically to zirconium, is removed during the ion exchange separation. Also, copper is not held by the resin. In addition, fuming the resin ash

with sulfuric acid removes all traces of nitrate, perchlorate, and iodide. Thus, in the analysis of most rock samples all interfering ions are removed by an ion exchange separation followed by the volatilization of boron as methyl borate followed, in turn, by the volatilization of osmium, chloride, iodide, nitrate, and perchlorate with hot sulfuric acid.

The Analysis of Niobium and Tantalum

On the basis of the previously described studies the following procedure is formulated for the determination of microgram quantities of niobium and tantalum in rocks.

Procedure

Sample preparation. Crush between 25 and 50 grams of fresh rock chips with a steel mortar and pestle to less than 80 mesh. Before weighing, mix the sample by repeated "rolling" on a sheet of weighing paper.

Decomposition of sample. Transfer up to 1.0 gram of sample to a 50 ml. polypropylene centrifuge tube and add 5.0 ml. of concentrated hydrochloric acid and 4.0 ml. of concentrated hydrofluoric acid. In the treatment of samples containing appreciable amounts of carbonate, first add dilute hydrochloric acid until the carbonate is decomposed, then warm to dryness and add the concentrated acids. Seal the tube and place it in a warm location for 24 hours. Swirl the mixture occasionally to aid the decomposition. When the decomposition is complete, add 11 ml. of water to the tube,

mix, and centrifuge. At this point the solution is ready to be added to the ion exchange column.

Ion exchange separation. Prepare an ion exchange column according to the procedure described on page 16. Wash the column with 20 ml. of 25/20 acid solution. Prime the column with enough 25/20 acid solution to give an aqueous level 2 or 3 inches above the resin bed. Pour the sample-bearing solution from the centrifuge tube into the column reservoir. The addition of the insoluble residue to the column greatly slows the rate of flow and may result in contamination of the sample. Wash the residue in the centrifuge tube with two 5 ml. portions of the 25/20 acid solution. Centrifuge after each wash and add the solution to the column reservoir immediately after the reservoir empties. Next, wash the reservoir and column with a total of 30 ml. of 25/20 acid solution. When all of the solution has passed through the column, remove the reservoir and wash the resin from the column into a polyethylene funnel containing a fine, low ash filter paper. The resin is readily flushed from the column by attaching a water line to the polyethylene nipple. Wash the resin with 30 ml. of water in 5 ml. portions to remove the hydrochloric and hydrofluoric acids.

Determination of niobium and tantalum. Dry the resin and ignite in a platinum crucible, first at a low temperature (about 400°C) then at 1100°C. Although platinum is an interference in both determinations, the ignition in platinum crucibles does not cause an interference in the analysis.

Add 1 ml. of 4N hydrochloric acid and 1 ml. of methanol to the residue. Warm to dryness on a steam bath to volatilize boron. Add 0.5 ml. of concentrated sulfuric acid to the residue and fume to dryness. Heat the crucible briefly in a bunsen flame to decompose traces of organic matter. Add 3 ml. of concentrated hydrofluoric acid. Slowly warm the solution to dryness. The temperature should be less than 50°C during this evaporation. Higher temperatures result in a loss of niobium and tantalum either by the volatilization of their fluorides or the formation of their pentoxides after reaching dryness. When dry, dissolve the residue in 1.5N hydrofluoric acid. The amount of hydrofluoric acid solution should be controlled so that a 2 ml. aliquot contains between 1 and 10 µg. of Ta_2O_5. For the determination of tantalum add a 2 ml. aliquot of the 1.5N hydrofluoric acid solution to a 50 ml. polypropylene centrifuge tube and follow the procedure outlined for the preparation of a Ta_2O_5 calibration curve (page 11). In the determination of niobium it is usually necessary to dilute a 1 ml. aliquot of the 1.5N solution to 25 ml. Transfer between 1 and 5 ml. of the diluted niobium solution to 50 ml. borosilicate beakers and warm to dryness. Add 1 gram of potassium pyrosulfate, fuse, and follow the procedure outlined for the preparation of a Nb_2O_5 calibration curve (page 6).

Results and Conclusions

A series of analyses were conducted to test the efficiency of the ion exchange separation and the reproducibility of the analytical procedure. Table V shows the results of replicate niobium determinations. The niobium contents of the standard granite, G-1, and diabase, W-1, are in close agreement with the values found by Grimaldi. The preferred spectrographic value of the standard granite is 27 ppm. Nb_2O_5 (Ahrens and Taylor, 1961), somewhat higher than the value given in Table V.

TABLE V

Results of Niobium Analysis

Sample	Number of Analyses	Average Nb_2O_5 (ppm.)	Standard Deviation	Range (ppm.)
ML-3 Carbonatite	10	540	17	510-570
W-7 Pyroxenite	6	8.9	1.3	7.2-10.4
G-1 Granite	3	22		
W-1 Diabase	3	9.6		

Table VI shows the result of replicate tantalum determinations. The preferred spectrographic values of 1.9 and 0.57 ppm. Ta_2O_5 for the standard granite and diabase are considerably lower than the values in Table VI, but the tantalum content of G-1 is in close agreement with the average tantalum content of granitic rocks (4.3 ppm. Ta_2O_5) reported by Vinogradov (1962). The tantalum content of

W-1 is higher than the Vinogradov's average value of 0.60 ppm. Ta_2O_5. The values of Ahrens and Taylor and Vinogradov are the result of spectrographic determinations that envolved a preliminary concentration of tantalum in an oxalate medium. It was noted earlier (page 9) that microgram amounts of tantalum tend to hydrolyze in oxalate solution. Hydrolysis of tantalum during the preliminary concentration probably accounts for the low values reported by these authors.

TABLE VI

Results of Tantalum Analysis

Sample	Number of Analyses	Average Ta_2O_5 (ppm.)	Standard Deviation	Range (ppm.)
ML-3 Carbonatite	10	21	1	18-23
IH-3 Uncomphagrite	6	4.4	0.6	3.8-6.5
W-7 Pyroxenite	6	0.46	0.24	0.32-0.60
G-1 Granite	3	4.3		
W-1 Diabase	3	1.8		

Impurities were added to 200 mg. samples of the carbonatite, ML-3, prior to the ion exchange separation. The effect of the added impurities on the tantalum analysis is shown in Table VII.

TABLE VII

Analysis of ML-3 with Added Impurities

Element	Amount Added (μg.)	Ta_2O_5 Found (ppm.)	Error (ppm.)
Re (VII)	500	19	-2
B (III)	"	23	+2
Cr (III)	"	23	+2
Sb (III)	"	21	0
Sn (IV)	"	18	-3
Mo (IV)	"	20	-1
V (V)	"	21	0
Pt (IV)	"	19	-2
Os (III)	"	19	-2
Pd (IV)	"	21	0
W (VI)	"	20	-1
Hf (IV)	5000	21	0
Zr (IV)	"	19	-2
Cu (II)	"	20	-1
Th (IV)	"	23	+2
Ce (IV)	"	19	-2

The errors produced by the addition of the 16 interfering elements fall within the range of experimental error shown in Table VI. The effect of larger amounts of impurities was not determined, but in a 200 mg. sample 500 μg. of an added impurity is equivalent to 0.25% and 5000 μg. of an

impurity is equivalent to 2.5%. Few rocks contain the interfering elements in excess of these amounts.

In conclusion, all of the elements interfering in the analysis of niobium and tantalum are removed by the procedure just outlined. The analytical procedure offers a highly sensitive and selective method for the determination of trace amounts of niobium and tantalum in rocks.

PART II

THE NIOBIUM AND TANTALUM CONTENT OF SOME ALKALI IGNEOUS ROCKS

Alkali igneous complexes are characterized by silica-deficient, alkali-rich conditions that lead to the formation of rather unusual rock types. Rocks range in composition from ultramafics to trachytes, syenites and nepheline syenites. Pyroxene-feldspathoid rocks are common and late intrusions of carbonate are usually present. The complexes are often surrounded by altered wall-rock referred to as fenite. The structural features of these complexes are distinctive. They are more or less circular or elliptical in shape and relatively small in size. The largest known complex is the Chibina complex of Russia which has an outcrop area of 250 square miles. A more typical example is the complex at Magnet Cove, Arkansas, (see Figure 12) which covers an area of about 4.6 square miles. In general, the complexes appear to occupy the necks of extinct volcanoes and were probably formed during the last stages of volcanic activity.

Many hypotheses concerning the origin of alkali igenous complexes have appeared in the literature. The proposed genetic processes include: 1. desilication of normal magmas by assimilation of limestone (Daly, 1910, 1918; Shand, 1945); 2. alteration of normal rocks by metamorphism

or metasomatism (Smyth, 1913, 1927; von Eckerman, 1948; Tilley, 1957); 3. fusion and recrystallization of a limy shale-evaporite sequence (Jensen, 1908); 4. differentiation of a peridotite magma (Holmes, 1932; Holmes and Harwood, 1932; Strauss and Truter, 1951); 5. differentiation of an undersaturated olivine basalt magma (Kennedy, 1933; Barth, 1936; Erickson and Blade, 1963).

Late carbonate intrusions, or carbonatites, are often associated with alkali igneous complexes. Rowe (1958) defines a carbonatite as a "rock that consists of 50 per cent or more carbonatite and is not of sedimentary or biogenic origin. The term is commonly used by African geologists to refer to carbonate rocks of volcanic origin. Some geologists use the term to refer to carbonate rock in an alkaline roxk complex regardless of its origin." Carbonatites are of particular economic interest because they are greatly enriched in rare elements such as barium, strontium, niobium, titantium, zirconium, phosphorous, and the rare earths. The Mountain Pass carbonatite described by Olsen et. al. (1954) is the largest rare earth deposit in the world and De Kun (1962) estimates that carbonatites contain 98.5% of the world's niobium reserves, consisting of more than 10,000,000 metric tons of niobium.

There is disagreement as to the origin of carbonatites. Some observers believe that carbonatites are hydrothermal deposits (Bowen, 1924, 1926; Heinrich and Levinson, 1963).

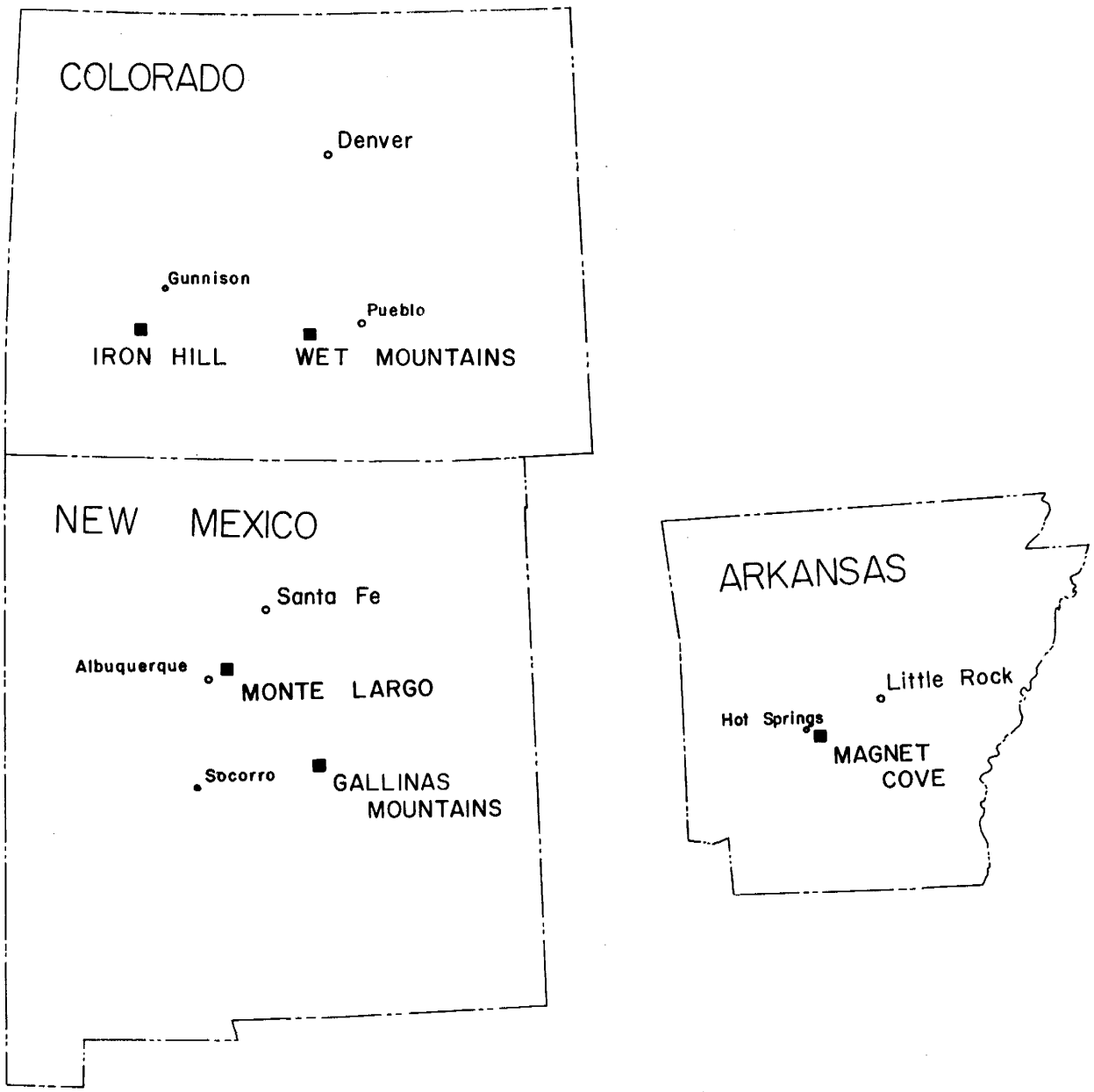

Figure II. Index Map of Sample Localities

Others believe that carbonatites are magmatic intrusions (Brogger, 1921; Turner and Verhoogen, 1960; Erickson and Blade, 1963). The field and geochemical evidence from the areas studied in this thesis suggests that the carbonatites were emplaced as volatile-rich carbonate magmas.

Although there are some data available concerning the niobium content of alkali igneous rocks, the literature is almost barren of information concerning the tantalum content of these rocks. In this paper the results of 52 rock analyses for niobium and tantalum are given. The samples include a wide variety of alkali igneous rock types from six geographical areas within the United States (see Figure 11). The areas sampled include: 1. Magnet Cove, Arkansas; 2. Monte Largo, New Mexico; 3. Wet Mountains, Colorado; 4. Iron Hill, Colorado; 5. Gallinas Mountains, New Mexico; 6. Mountain Pass, California.

Magnet Cove

The Magnet Cove alkali igneous complex is located in central Arkansas 12 miles east of Hot Springs. The geochemistry and petrology of the area have been studied in detail by Erickson and Blade (1963) and Figure 12 is a simplified geologic map based on their work. The complex is roughly circular and covers an area of 4.6 square miles. The undersaturated rocks are intruded into Paleozoic sediments ranging from Ordovician to Mississippian in age. Erickson and Blade believe the igneous activity took place during

Mesozoic time, probably extending from the Triassic to the Cretaceous period. The relative ages of the rock units from oldest to youngest are: 1. phonolites and trachytes; 2. jacupirangite; 3. alkalic syenites; 4. ijolites; 5. carbonatite, dike rocks, and veins.

Seven powder samples from the Magnet Cove complex were supplied by R. L. Erickson. They include: 1. sphene-nepheline syenite (MC-1); 2. garnet-nepheline syenite (MC-112); 3. jacupirangite (MC-173); 4. trachyte-phonolite (MC-227); 5. biotite-garnet ijolite (MC-216); 6. garnet ijolite (L-17); and 7. carbonatite (L-304). The sample locations are shown in Figure 12 and a brief petrographic description of the samples is included in Appendix I.

According to Erickson and Blade the sphene-nepheline syenite (MC-1) is a medium-grained rock consisting mainly of orthoclase, nepheline, and zoned pyroxenes. Essentially all of the niobium is concentrated in accessory sphene that contains 0.7% Nb.

The garnet-nepheline syenite (MC-112) is a coarse-grained variety of a garnet-pseudoleucite syenite. The two rock units together comprise 24.5% of the exposed complex. The essential minerals are orthoclase, nepheline, and pyroxene. Accessory garnet and perovskite are the major niobium-bearing minerals and contain 0.66% Nb and 0.3% Nb respectively.

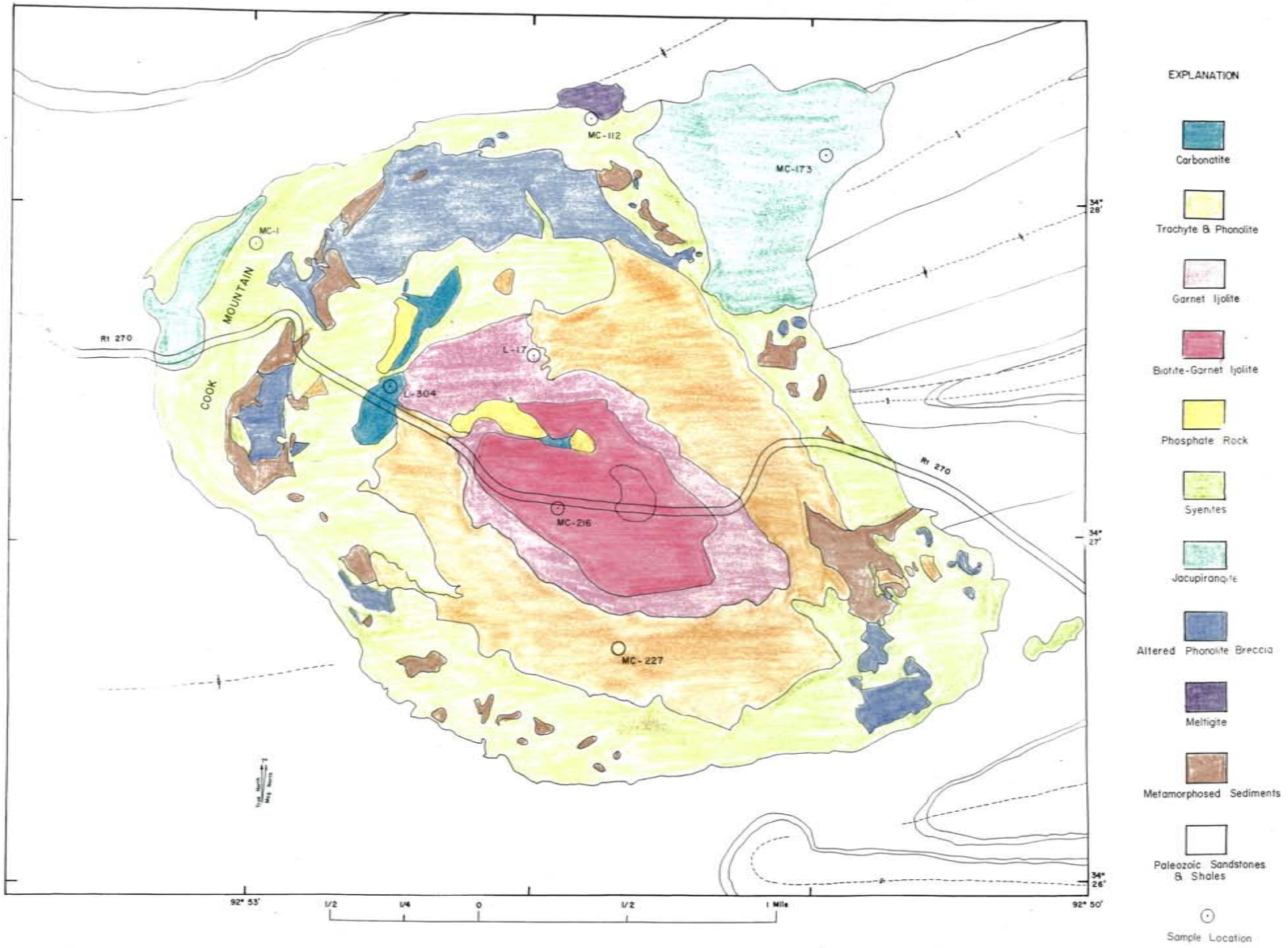

Figure 12 Geologic Map of the Magnet Cove Area after R.L. Erickson and L.V. Blade

The essential minerals of the jacupirangite (MC-173) are pyroxene and magnetite-ilmenite. The major niobium-bearing minerals are sphene (0.1 to 0.15% Nb) and perovskite (0.3% Nb).

Several varieties of trachyte and phonolite are found at Magnet Cove. The sample supplied by Erickson (MC-227) is an alkalic trachyte composed of sodic orthoclase and albite. Sphene from the sample contains 0.01% Nb and is the major niobium-bearing mineral.

The biotite-garnet ijolite (MC-216) and the garnet ijolite (L-17) are gradational. Pyroxene, nepheline, and biotite are the essential minerals and perovskite (0.36 to 0.9% Nb), sphene (0.01% Nb), and garnet (0.03%Nb) are the niobium-bearing minerals.

The carbonatite (L-304) is composed of medium to coarse-grained calcite with scattered zones enriched in apatite, brown monticellite, magnetite, black perovskite, green biotite, pyrite, and kimzeyite. The carbonatite weathers to a porous rock, mapped as "Phosphate Rock" in Figure 12, which is composed of residual minerals from the carbonatite in a matrix of secondary apatite. The difficulty in obtaining a representative sample of the carbonatite was clearly shown by Fryklund, Harner, and Kaiser (1954). Of 21 samples taken from the carbonatite, only 6 contained niobium in detectable amounts, yet they found the average content of the carbonatite to be 0.014% Nb_2O_5. The niobium in the carbonatite and

phosphate rock is concentrated in the perovskite (up to 9.2% Nb), kimzeyite (.5% Nb), and anatase (6.8% Nb).

The niobium and tantalum content of the Magnet Cove samples is given in Table VIII. The results of the niobium analysis are in close agreement with the spectrographic analyses of Erickson and Blade, but they were unable to detect tantalum in the samples by their spectrographic methods.

TABLE VIII

Niobium and Tantalum Content of Rocks from the Magnet Cove Area

Sample	Number of Analyses	Nb_2O_5 (ppm.)	Nb_2O_5 (E&B)*	Ta_2O_5 (ppm.)	Nb/Ta
MC-227 Trachyte	3	130	140	16	6.9
MC-173 Jacupirangite	3	270	28	40	5.8
MC-112 Garnet-nepheline syenite	2	140	140	11	11
MC-1 Sphene-nepheline syenite	2	110	120	6.8	14
L-17 Garnet ijolite	2	70	28	4.3	14
MC-216 Biotite-garnet ijolite	1	78	71	4.1	17
L-304 Carbonate	1	71	80	1.0	63

* Erickson and Blade

Although the number of analyses is small and perhaps not representative of the area, those samples analyzed show an increasing enrichment of niobium over tantalum in the later forming rocks. The rock sequence, the average Nb/Ta ratios, and the estimated standard deviations of the ratios (see Appendix III) are:

trachyte (6.9 $\pm$0.3), jacupirangite (5.8 $\pm$0.3)→ nepheline syenites (12 $\pm$1)→ijolites (15 $\pm$2)→carbonatite (63).

The Nb/Ta ratio for the complex as a whole can be estimated on a weighted basis by multiplying the Nb/Ta ratio of a rock unit by its outcrop area. The sum of the weighted ratios divided by the total outcrop area represented gives the ratio of the complex. Table IX shows these calculations for the Magnet Cove Area.

TABLE IX

Calculations of the Nb/Ta Ratio of the Magnet Cove Complex

Sample	Outcrop Area (%)	Nb/Ta	Weighted Nb/Ta
Trachyte	20	6.9	138
Jacupirangite	10	5.8	58
Garnet-nepheline syenite	25	11	275
Sphene-nepheline syenite	7	14	98
Garnet ijolite	5	14	70
Biotite-garnet ijolite	7	17	119
Carbonatite	2	63	126
	76		884

The average Nb/Ta ratio of the Complex is 884/76 = 11.6

Monte Largo

In studying the Precambrian rocks of the Monte Largo area located 22 miles northeast of Albuquerque, New Mexico, Lambert (1961) observed a carbonate dike and a melteigite dike or sill (see Figure 13). The age of the two intrusions is not certain, but they are younger than the Precambrian rocks of the area and older than the Pennsylvanian rocks west of the Golden Fault.

The carbonatite dike occurs in a brecciated area. The dike is 1 to 2 feet thick and can be traced for a distance of approximately 200 feet. The carbonatite is a dark grey aphanitic rock containing calcite, dolomite, magnetite and apatite in essential amounts.

Optical and X-ray examination failed to show the presence of niobium or tantalum minerals. Analysis of the magnetite showed 0.013% Nb_2O_5, but this is not sufficient to account for the niobium content of the rock. The niobium and tantalum may be concentrated in fine-grained, possibly metamict, pyrochlore. The occurence of very small pyrochlore grains in carbonatites has been reported by Rowe and van der Veen (1963).

The breccia in which the carbonatite occurs is an explosion breccia according to Lambert and is composed of Precambrian rock and mineral fragments of varying size cemented by calcite and to a lesser degree dolomite.

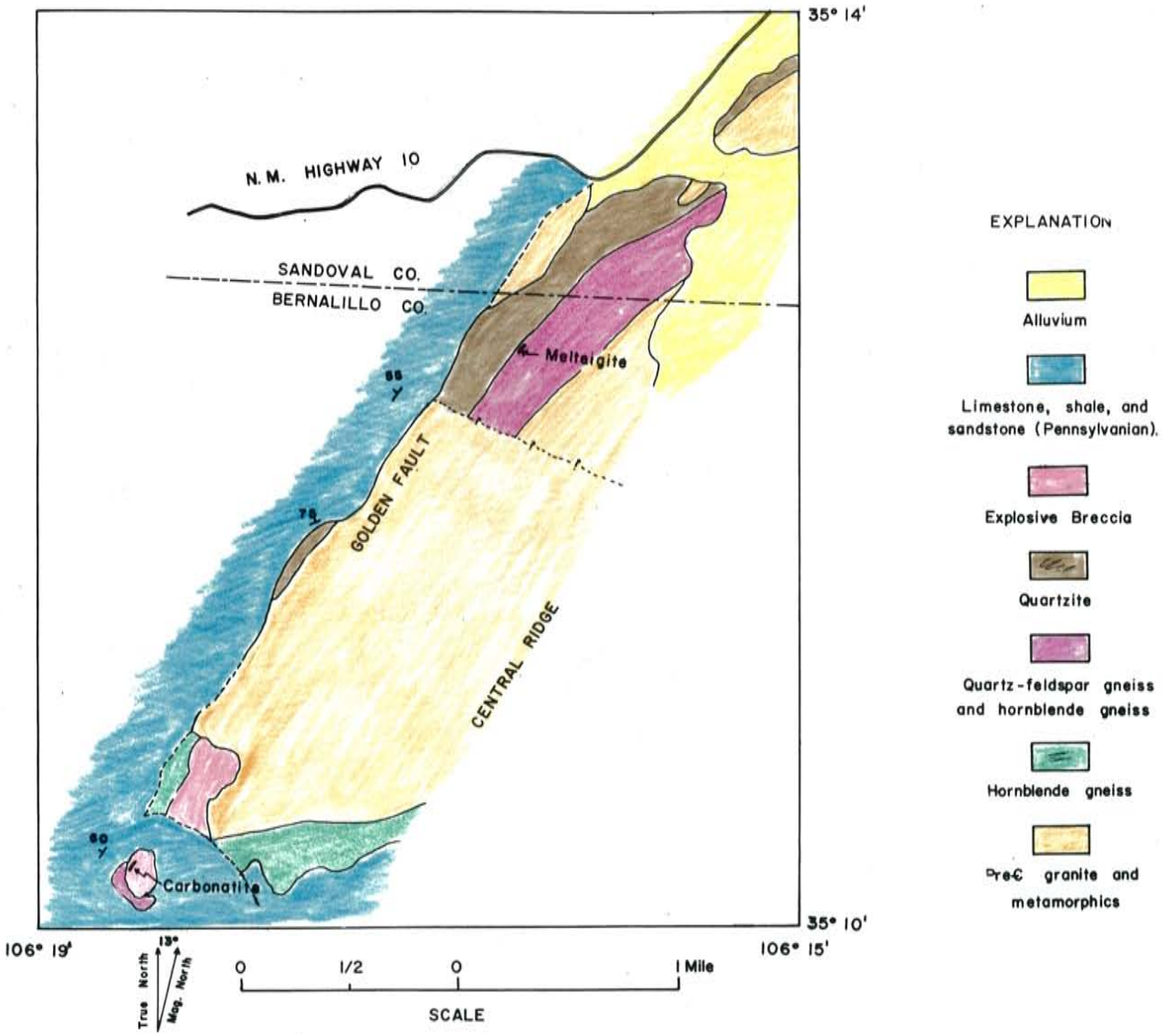

Figure 13. Geologic Map of Part of the Monte Largo Area after P. W. Lambert

The amount of carbonate present is highly variable. Subhedral magnetite is abundant in the breccia and apparently was introduced along with the carbonate mineralization.

A melteigite dike or sill outcrops in a small area $2\frac{1}{2}$ miles northeast of the carbonatite. The body is several feet thick and occurs in a hornblende gneiss. It consists of pyroxene, nepheline, and a prismatic mineral believed to be wollastonite. Accessory sphene is the likely niobium and tantalum-bearing mineral. Table X shows the niobium and tantalum content of the rocks from the Monte Largo area. Samples ML-3, ML-4, and ML-8 were taken at approximately 40 foot intervals along the carbonatite dike. The breccia sample was taken 100 feet east of the carbonatite.

TABLE X

Niobium and Tantalum Content of Rocks from the Monte Largo Area

Sample	Number of Analyses	Nb_2O_5 (ppm.)	Ta_2O_5 (ppm.)	Nb/Ta
ML-3 Carbonatite	10	540	21	22
ML-4 "	4	570	24	20
ML-8 "	2	540	23	20
ML-6 Carbonate breccia	2	92	7.2	11
ML-12 Melteigite	2	440	23	16

In contrast with the carbonatite at Magnet Cove, the niobium and tantalum content of the Monte Largo carbonatite appears to be fairly uniform. Undoubtedly, this is due to the aphanitic nature of the dike which greatly reduces the problem of obtaining a representative sample. The tantalum content of the carbonatite is unusually high and, as a result, the Nb/Ta ratio of the rock is relatively low in comparison with carbonatites from other areas.

If the carbonatite (avg. Nb/Ta = 21 $\pm$1) and melteigite (Nb/Ta = 16 $\pm$1) are associated with the same source magma, the melteigite, on the basis of the Magnet Cove and Wet Mountains rock sequences, is probably earlier than the carbonatite. Although slight, there is a definite enrichment of niobium over tantalum in the carbonatite dike which is in agreement with the findings at other areas. The high niobium content of the breccia 100 feet from the dike suggests that the niobium was in a very mobile state. The impregnation of the breccia may have been metasomatic or the niobium may have been carried by a hydrothermal solution associated with the late stage of crystallization of a "wet" carbonate magma. Metasomatism or hydrothermal activity could also account for the subhedral magnetite and carbonate cement found in the breccia.

Wet Mountains

There are two genetically related alkali igneous complexes in the Wet Mountains 13 miles north of Westcliff, Colorado. The area is presently being examined by Parker and Hildebrand (1963) and Figure 14 is a copy of their preliminary map. The McClure Mountain complex is roughly circular and occupies an area of 20 square miles. The smaller Gem Park complex to the southwest occupies an area of 2 square miles. Both are intruded into Precambrian granite and metamorphic rocks. Parker and Hildebrand believe the age of the alkali rocks is late Precambrian. The relative age of the rock units from oldest to youngest is: pyroxene-olivine-plagioclase rocks, biotite-hornblende syenite, mafic nepheline-bearing rocks, nepheline syenite, and carbonatite dikes.

The unit mapped as pyroxene-olivine-plagioclase rocks contains rocks of highly varying grain size and composition. Pyroxenites, gabbros, and andesites are found within the unit. Five samples of the pyroxene-olivine-plagioclase rocks were analyzed and examined briefly in thin section.

The samples, W-18a and W-18b, were taken from the same outcrop approximately 100 feet apart. Both are pyroxenites composed primarily of augite with minor amounts of magnetite and plagioclase. The pyroxenite, W-7, is similar in composition to W-18, but, in addition, W-7 contains hornblende and calcite.

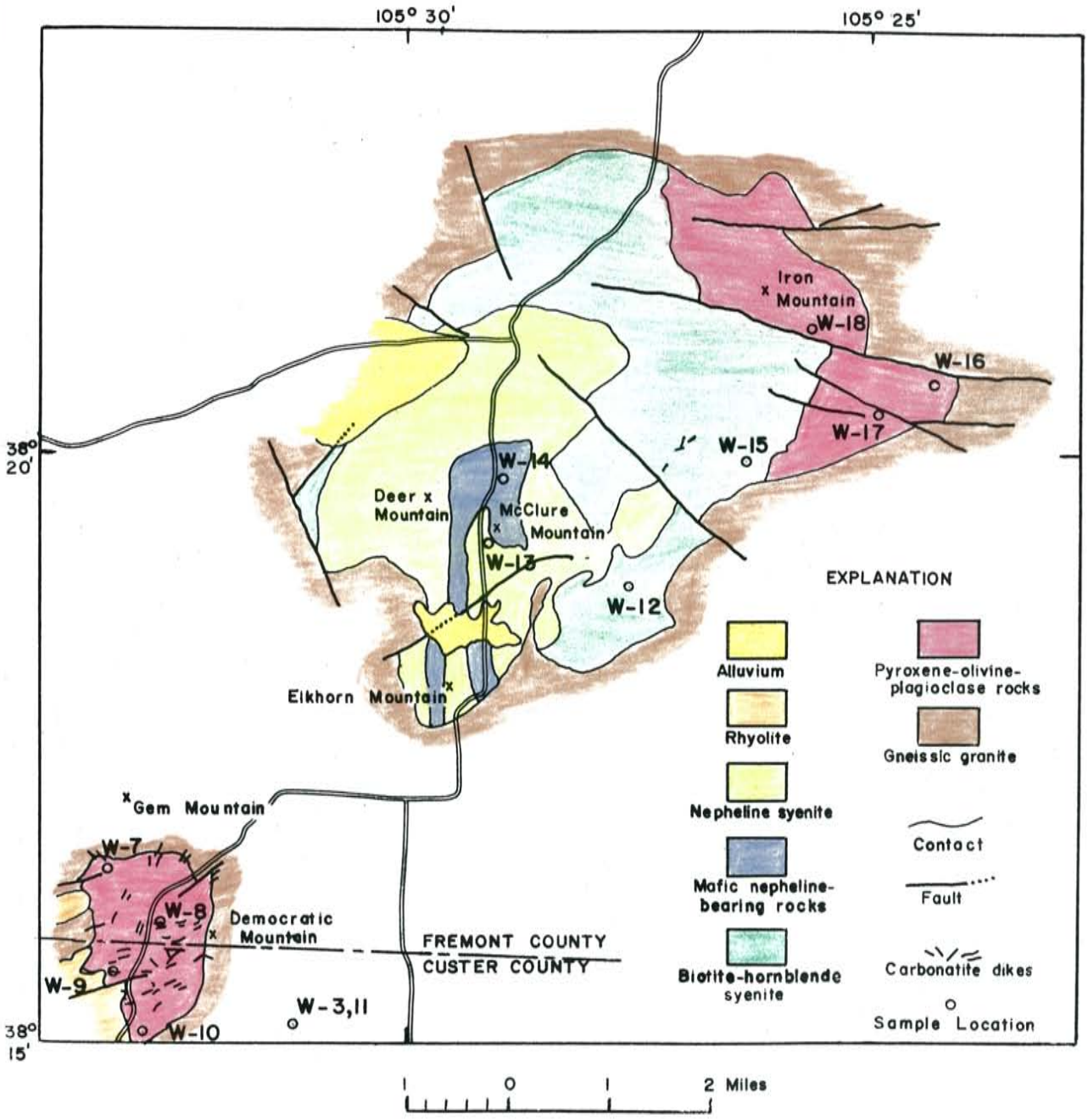

Figure 14 Geologic Map of the Wet Mountain Area, Colorado, after R. L. Parker and F. A. Hildebrand

The essential minerals of the gabbro, W-16, are ophitic anorthite and augite. The gabbro, W-10, is composed primarily of bytownite and diopside or augitic-diopside. W-9 is a gabbro sample collected approximately 100 feet from a carbonatite dike. It is similar to W-10 except it is altered and partially replaced by calcite.

The samples of biotite-hornblende syenite (W-12, W-15) are very coarse-grained and contain orthoclase, green and brown hornblende, and biotite.

The sample from the unit mapped as "Mafic nepheline-bearing rocks" (W-14) is a hornblende ijolite. The essential minerals of the rock are nepheline, pyroxene and hornblende.

The sample from the unit mapped as "Nepheline syenite" (W-13) may be classified as a biotite-hornblende-nepheline syenite.

The carbonatite dike samples (W-8, W-17) consist predominately of calcite and dolomite with limonite, magnetite, apatite, muscovite, actinolite-tremolite, and quartz present in varying amounts.

Four samples were collected at a prospect pit 1 mile southeast of the Gem Park complex. The samples consist of a crocidolite carbonatite, fenite, and replaced Precambrian granite. The granite sample (W-3c) collected 50 feet from the prospect, is partially replaced by calcite and dolomite. W-11 is a sample of the granite that has been almost completely replaced by calcite and to a lesser degree dolomite and ankerite. A crocidolite carbonatite (W-3a) is exposed in

the prospect pit. The sample consists primarily of dolomite and crocidolite. The fourth sample (W-3b) is a fenite in which quartz has been replaced by crocidolite. The mineral sequence indicated by the four samples is: preC granite replaced by carbonate followed by crocidolite.

The niobium mineralization definitely accompanied the carbonate and possibly accompanied the crocidolite as well. The granites replaced by carbonate (W-3c, W-11) show an enrichment in niobium (see Table XI). In addition, the crocidolite replaced granite (W-3b) shows high enrichment in niobium, and a crocidolite vein sample (W-2) taken approximately 100 feet south of location W-8, also has a nigh niobium content. This tends to indicate an association of niobium and crocidolite, but it is also possible that: 1. the niobium in the crocidolite vein is related to the nearby carbonatite (this is not likely since the crocidolite is later than the carbonate at locality W-8) or 2. the fenite was formed in two steps, first, a selective replacement of quartz in the Precambrian granite by carbonate and associated niobium, then a selective replacement of carbonate by crocidolite.

The niobium and tantalum in the carbonatites is probably concentrated in pyrochlore or possibly perovskite. A positive identification was not made since these minerals are not sufficiently abundant to be readily identified in thin section. The niobium and tantalum contents of 18 samples from the Wet Mountains complex are given in Table XI.

TABLE XI

Niobium and Tantalum Content of Rocks from the Wet Mountains Area

Sample	Number of Analyses	Nb_2O_5 (ppm.)	Ta_2O_5 (ppm.)	Nb/Ta
W-2 Crocidolite vein	1	220	5.5	34
W-3a Crocidolite carbonatite	1	2800	11	220
W-3b Fenite	1	350	2.5	120
W-3c Pre€ granite	1	480	2.0	210
W-7 Pyroxenite	6	8.9	0.46	17
W-8 Carbonatite	2	68	3.1	19
W-9 Gabbro	1	36	1.5	21
W-10 Gabbro	1	5.8	2.1	2.4
W-11 Replaced granite	2	47	2.5	16
W-12 Biotite-hornblende syenite	1	160	10	14
W-13 Nepheline syenite	2	120	6.0	17
W-14 Hornblende ijolite	3	160	6.3	22
W-15 Biotite-hornblende syenite	2	50	2.8	15
W-16 Gabbro	2	9.0	2.3	3.3
W-17 Carbonatite	2	55	1.0	48
W-18a Pyroxenite	2	5.6	2.1	2.3
W-18b Pyroxenite	1	5.0	0.88	4.8

The analytical data indicate that the late-forming rocks of the Wet Mountains complex are enriched in niobium over tantalum. This is in agreement with the finding at Magnet Cove. The rock sequence and average Nb/Ta ratios are:

pyroxene-olivine plagioclase rocks (3.2 ± 0.9) →
biotite-hornblende syenite (15 ± 2) →
mafic nepheline-bearing rocks (22 ± 2) →
nepheline syenite (17 ± 2) → carbonatites (95 ± 10).

The gabbro, W-9, and the pyroxenite, W-7, were omitted in averaging the Nb/Ta ratio of the pyroxene-olivine-plagioclase rocks. W-9 is a sample taken near a carbonatite dike and shows contact enrichment in niobium. Although a carbonatite dike was not observed in the vicinity of W-7, the anomalously high Nb/Ta ratio and the partial replacement of the sample by carbonate suggest that the pyroxenite might be a contact rock and, therefore, not a representative sample.

The Nb/Ta ratios of the carbonatites show a very wide variation ranging from 19 to 220. This is attributed to the wide range in the niobium content, 55 to 2800 ppm., as compared with the relatively small range of the tantalum content, 1 to 11 ppm. There is only a slight enrichment of tantalum in the carbonatite samples that show an enrichment in niobium.

As previously mentioned, the gabbro, W-9, shows an enrichment in niobium. The sample was taken approximately 50 feet from a carbonatite dike. In addition, the fenite sample,

W-3b, taken a few feet from the crocidolite carbonatite and the replaced granite, W-3c, taken 50 feet from the carbonatite also show enrichment in niobium. As in the case of the Monte Largo breccia, the carbonate replacement and enrichment of niobium in the country rock suggests the rock was permeated by fluids emanating from the carbonatite magma.

The calculation of the Nb/Ta ratio for the complex on a weighted basis is given in Table XII.

TABLE XII

Calculation of the Nb/Ta Ratio of the Wet Mountains Complex

Rock Unit	Number of Samples	Outcrop Area (%)	Average Nb/Ta	Weighted Nb/Ta
Pyroxene-olivine-plagioclase rocks	4	26	3.2	83
Biotite-hornblende syenite	2	40	15	600
Mafic nepheline rocks	1	5	22	110
Nepheline syenite	1	29	17	492
		100		1285

The Nb/Ta ratio of the complex as a whole calculated by dividing 1285/100 is 12.8, a ratio similar to that of the Magnet Cove complex.

Iron Hill

The Iron Hill alkali igneous complex is located just east of Powderhorn Valley on the northern flank of the San Juan Mountains approximately 25 miles south-southwest of Gunnison, Colorado. The geology of the area has been studied in detail by Larsen (1941) and Figure 15 is a simplified version of his map. For clarity, 63 carbonatite dikes are omitted in Figure 15.

The alkali rocks have been intruded into Precambrian rocks and are believed to be Precambrian in age. The oldest rock within the complex is the large carbonatite mass that forms Iron Hill. Pyroxenite veinlets cut the massive carbonatite near the contacts, but carbonatite dikes similar in composition to the main carbonatite are abundant in the pyroxenite. The formation of the main carbonatite was followed, in order, by the intrusion of uncompahgrite, pyroxenite, ijolite, sodium-rich syenite, nepheline syenite, and carbonatite dikes. Twelve thin sections of the major rock types were briefly examined (see Appendix I). A much more complete study of the rock units is given by Larsen.

The uncompahgrite sample (IH-3) is a partially altered rock containing chiefly melilite, garnet, and pyroxene. Perovskite and calcite appear to have been introduced after the formation of the rock.

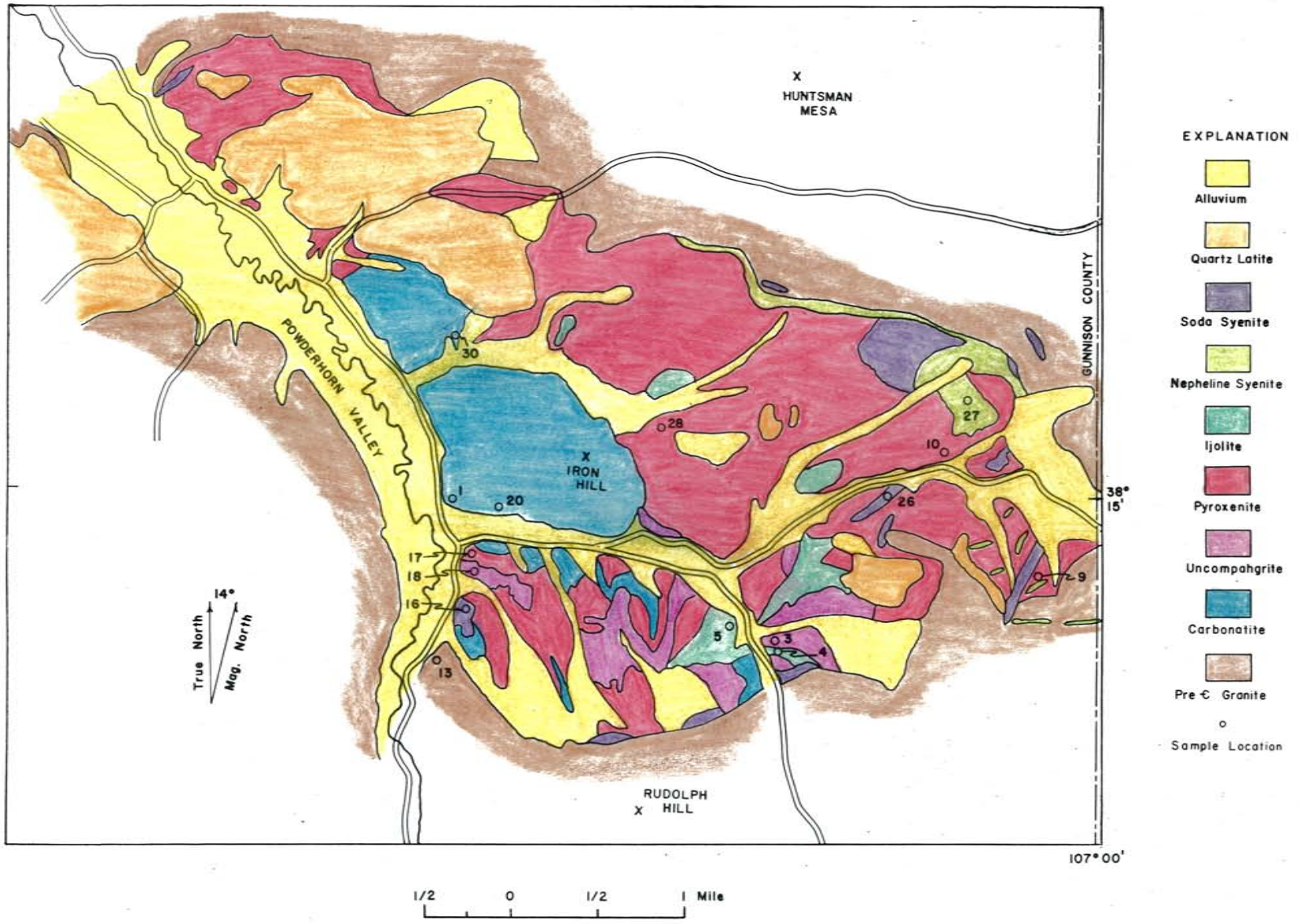

Figure 15. Geologic Map of the Iron Hill Area, Colorado, after E. S. Larsen

Larsen states that "one of the most prominent characteristics of the pyroxenite is the variability." IH-10 is a nepheline pyroxenite, or melteigite according to Johannsen (1938), composed of augite, nepheline, sphene, and apatite. Interstitial carbonate may indicate the presence of a nearby carbonatite dike. The high Nb/Ta ratio (40) of the sample also suggests that the sample is a contact rock.

A second pyroxenite sample (IH-9) was examined using a binocular microscope and oil immersion techniques. It contains predominately augite and biotite altered, in part, to chlorite.

Like the pyroxenite, the unit mapped as ijolite shows a wide variation in composition. Larsen states that samples range from urtite, through ijolite, to melteigite and, in addition, include jacupirangite, juvite, and malignite. IH-4 is a coarse-grained melteigite that consists of green augite and unaltered nepheline. Another sample from the unit mapped as ijolite (IH-5) is a garnet melteigite containing mainly pyroxene, garnet, and nepheline.

The soda syenite samples (IH-16, IH-26) are composed of perthite and vein-like zones of green aegirine-augite. The nepheline syenite (IH-27) is predominately composed of alkali feldspars, nepheline, with some biotite and pyroxene.

IH-13 is a sample of Precambrian granite collected near the contact with the alkali complex. The granite is coarse-grained containing quartz, orthoclase, albite, microcline,

and perthite. Irregular veinlets of amphibole cut the sample.

The carbonatite samples from the area are composed of dolomite or calcite and phlogopite. Minor and accessory constituents include biotite, apatite, magnetite, hematite, limonite, perovskite, pyrite, chalcopyrite, and riebeckite.

The niobium and tantalum content of 16 samples from the Iron Hill complex is given in Table XIII.

The results in Table XIII show that the Nb/Ta ratios of the silicate rocks at Iron Hill are, with a few exceptions, considerably higher than those of the Magnet Cove, Monte Largo, and Wet Mountains areas. Also, there does not appear to be a clear relationship between the relative ages of the Iron Hill rocks and the Nb/Ta ratios. Many of the analyzed samples show signs of alteration and may, in fact, represent "contact" rocks enriched in niobium by the action of late fluids associated with the carbonatite dikes that cut the complex. The enrichment of niobium in rocks bordering carbonatite dikes was demonstrated in other areas. At Iron Hill, the soda syenite sample (IH-16) was collected approximately 150 feet north of an exposed carbonatite dike and shows a very high Nb/Ta ratio. The enrichment of niobium in the granite (IH-13) near the alkali complex is further evidence of a metasomatic or hydrothermal emplacement of the niobium. In general, there is a small enrichment of tantalum in the samples that show a high niobium content indicating that some tantalum accompanies the niobium.

TABLE XIII

Niobium and Tantalum Content of Rocks from the Iron Hill Area

Sample	Number of Analyses	Nb_2O_5 (ppm.)	Ta_2O_5 (ppm.)	Nb/Ta
IH-1 Carbonatite	2	84	2.5	29
IH-3 Uncompahgrite	6	130	4.3	26
IH-4 Melteigite	2	43	1.4	26
IH-5 Garnet melteigite	1	200	10	17
IH-9 Altered pyroxenite	1	19	0.75	21
IH-10 Melteigite	2	140	3.3	40
IH-13 Pre€ granite	2	95	1	81
IH-16 Soda syenite	1	160	2.5	55
IH-17 Carbonatite dike	2	340	15	19
IH-18 " "	2	220	3.0	63
IH-20 Carbonatite (light zone)	2	230	4.0	49
IH-20 Carbonatite (dark zone)	2	300	5.0	51
IH-26 Soda syenite	1	16	1.4	9.8
IH-27 Nepheline syenite	2	75	3.1	21
IH-28 Carbonatite dike	1	7.5	0.6	11
IH-30 Carbonatite	1	1000	16	53

Table XIV shows the calculation of the average Nb/Ta ratio on a weighted basis. Because of the small number of samples and the widely varying ratios of the complex the calculated ratio may not be representative.

TABLE XIV

Calculation of the Nb/Ta Ratio of the Iron Hill Complex

Rock Unit	Number of Samples	Outcrop Area (%)	Average Nb/Ta	Weighted Nb/Ta
Carbonatite	6	5.9	40	236
Uncompahgrite	1	5.9	26	125
Ijolite	2	4.0	18	72
Pyroxenite	2	79.2	34	2690
Soda syenite	2	2.0	39	78
Nepheline syenite	1	4.0	21	84
		100.0		3285

The Nb/Ta ratio of the complex as a whole is 32.9, approximately three times greater than the ratios of the Magnet Cove and Wet Mountains areas which have comparable outcrop dimensions.

Other Areas

Gallinas Mountains

The Gallinas Mountains are located about 50 miles east of Socorro, New Mexico, and 12 miles southwest of Corona, New Mexico (see Figure 11). Part of the Gallinas Mountains were mapped by Kelley (1949). More recently Perhac (1960) made

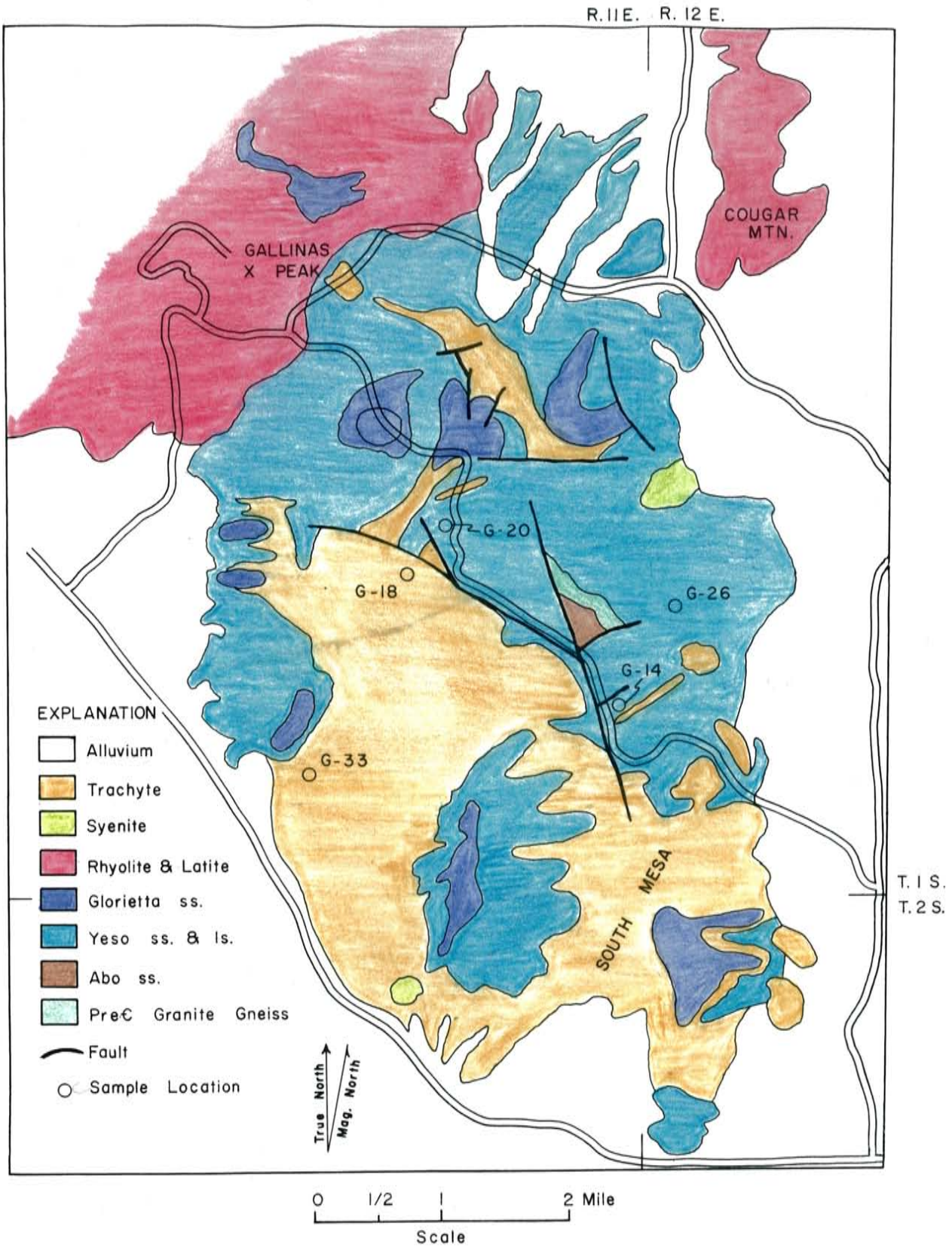

Figure 16. Geologic Map of the Gallinas Mountains Area after R. Perhac

a detailed study of the entire area and Figure 16 is a simplified version of his map. The Gallinas Mountains are a large domal uplift consisting of Precambrian granite overlain by 2000 feet of lower Permian sediments. The sediments are intruded by alkaline rocks of Tertiary age. The intrusions are predominately trachytes and syenites, but intrusive bodies of rhyolite and latite crop out in the northern part of the area. There are numerous copper-fluorite deposits containing the rare earth mineral bastnaesite. In 1954-55 60 tons of bastnaesite concentrate were produced from the Conqueror No. 9 workings (Griswold, 1959).

Five samples from the area were analyzed and briefly examined microscopically (see Appendix I). G-18 is a trachyte sample composed almost entirely of altered feldspar. G-33 is another trachyte similar to G-18, but fresher. Also, an andesite dike sample (G-20) and two fluorite samples were collected and analyzed. G-14 is a fluorite-barite rock from the Red Cloud bastnaesite deposit. G-26 is a sample of fluorite rock collected from a small prospect pit.

The niobium and tantalum content of the 5 samples from the Gallinas Mountains is given in Table XV.

The Nb/Ta ratios of the trachytes are in close agreement with the ratio of the trachyte from Magnet Cove. The similar ratios of the andesite dike and trachytes may indicate a close genetic relationship between the dike and the trachyte-syenite intrusive.

TABLE XV

Niobium and Tantalum Content of Rocks from the Gallinas Mountains Area

Sample	Number of Analyses	Nb_2O_5 (ppm.)	Ta_2O_5 (ppm.)	Nb/Ta
G-14 Fluorite-barite rock	2	14	0.2	60
G-18 Trachyte	1	28	3.2	7.5
G-20 Andesite dike	1	26	3.1	7.2
G-26 Fluorite rock	1	12	0.3	34
G-33 Albite trachyte	1	13	2.2	5.0

The fluorite-rare earth mineralization, believed to be of low temperature hydrothermal origin by Perhac, is almost certainly associated with the trachyte-syenite intrusion. The Nb/Ta ratios of the two fluorite rocks analyzed are relatively high, but this apparently represents a depletion in tantalum rather than an enrichment in niobium. The relative enrichment of niobium over tantalum in the late phases of crystallization of the alkali rocks is consistent with the finding at the other areas studied.

Mountain Pass

The Mountain Pass carbonatite and associated alkali igneous rocks are located in Southern California about 30 miles east of Baker near the Nevada-California boundary. The geology of the complex has been described by Olsen et. al. (1954). Various syenites and granites, a shonkinite, and a relatively large carbonatite mass have been intruded into Precambrian

granite, gneiss, and schist. Carbonatite dikes or veins similar in composition to the main carbonate mass cut the other rocks of the complex. Only one sample from the area was analyzed. The rock (MP-1) is from the Sulfide Queen carbonatite body and consists predominately of large barite phenocrysts in a matrix of calcite. The sample contains 110 ppm. Nb_2O_5 and 0.7 ppm. Ta_2O_5 giving a Nb/Ta ratio of 130. The high ratio of the carbonatite is consistent with the ratios found at other localities and suggests that there ma be an enrichment of niobium over tantalum in the late intrusions associated with the Mountain complex.

Results and Conclusions

Results:

The niobium and tantalum content of rocks from the 6 areas sampled has been presented in previous sections. Table XVI summarizes the results on the basis of rock type rather than geographical area. Also listed are the range and average niobium and tantalum content as well as the Nb/Ta ratios of the different rock types. Samples believed to have been enriched in niobium by the emplacement of nearby carbonatite bodies are not included.

In Table XVII the average Nb/Ta ratios of the alkali igneous rocks are compared to the ratios of similar rock types reported by Rankama and Sahama (1950).

TABLE XVI

Niobium and Tantalum Content of Some Alkali Igneous Rocks

Rock Type	Number Analyzed	Areas Represented*	Range Nb_2O_5 (ppm.)	Average Nb_2O_5 (ppm.)	Range Ta_2O_5 (ppm.)	Average Ta_2O_5 (ppm.)	Range Nb/Ta	Average Nb/Ta
Pyroxenites-gabbros andesites	5	W, G	5.0-26	10	.88-3.1	2.1	2.3-72	4.0
Jacupirangite	1	MC		270		40	5.8	5.8
Trachytes	3	MC, G	13-130	57	2.2-16	7.1	5.0-7.5	6.5
Syenites	2	W, IH	16-50	33	1.4-2.8	2.1	9.8-16	13
Nepheline syenites	4	MC, W, IH	75-440	220	3.1-11	6.7	11-21	16
Melteigites-ijolites	6	MC, ML, W, IH	43-440	100	1.4-23	4.7	14-26	20
Carbonatites	16	MC, ML, W, IH, MP	7.5-2800	470	0.6-24	8.5	11-220	58
Rare earth-fluorite rocks	2	G	12-14	13	0.2-0.3	0.25	34-60	47

* G = Gallinas Mountains

IH = Iron Hill

MC = Magnet Cove

ML = Monte Largo

MP = Mountain Pass

W = Wet Mountains

TABLE XVII

Comparison of Nb/Ta Ratios

Rock Type	Nb/Ta	
	Present Work	Rankama & Sahama
Ultrabasics and gabbros	4.0	16.0, 17.3
Basic alkalic rocks (trachytes)	6.5	8.3
Syenites	13	15
Nepheline syenite	16	387.5

In addition, De Kun (1960) listed the Nb/Ta ratio of carbonatites as 75, somewhat higher than the value of 58 reported in Table XVI, but his data is, in his words, "meager". The ultrabasic and basic rocks associated with alkali igneous complexes have a Nb/Ta ratio considerably lower than the average ratio reported by Rankama and Sahama (1950). The results for basic alkalic rocks and syenites are in fairly close agreement, but there is very poor agreement in the ratios of nepheline syenites. The average ratio reported by Rankama and Sahama (1950) is undoubtedly too high. Recent investigations have shown that the average Nb/Ta ratio of nepheline syenites from the Lovozero alkali complex, U.S.S.R., is 12.8 (Gerasimovskii et. al., 1959). Also, the average Nb/Ta ratio of nepheline syenites from the Vishnevyie alkali complex, U.S.S.R., is 12.0 (Es'Kova, 1959). The values reported in the Russian literature are in fairly close agreement with the values reported in this work.

It has been previously pointed out that the Nb/Ta ratios of the Wet Mountains and the Magnet Cove complexes are very similar, 12.8 and 11.6 respectively. This is in close agreement with the average Nb/Ta ratio of the Lovozero complex which is 11.4 according to Gerasimovskii et. al. The ratio of the Iron Hill complex is much higher, but this may be due to late metasomatic or hydrothermal enrichment of niobium in the analyzed samples. It is interesting to note that the average Nb/Ta ratios of the Magnet Cove, Wet Mountains, and Lovozero rocks are similar to the average ratio of igneous rocks, 11.4, reported by Rankama and Sahama (1950).

At Magnet Cove the early intrusions of trachyte and jacupirangite have ratios of 6.9 and 5.8, the intermediate intrusions of syenite and ijolite have ratios of 12 and 15, and the late intrusion of carbonatite has a ratio greater than 63. In the Wet Mountains the early basic rocks have a ratio of 3.2, the intermediate syenites and mafic nepheline-bearing rocks have ratios between 15 and 22, and the late carbonatite dikes have an average ratio of 81. The ratios of the melteigite and carbonatite in the Monte Largo area are consistent with the relative enrichment of niobium in late-forming rocks. The picture at Iron Hill is not as clear. The silicate rocks of the area show high and erratic ratios. The average Nb/Ta ratio of the carbonatite mass and dikes is greater, however, than that of the silicate rocks. The ratio of the Mountain Pass carbonatite is almost certainly higher than the older

associated rocks. The high ratios of the rare earth-fluorite deposits of the Gallinas Mountains and the crocidolite vein of the Wet Mountains are further evidence of a relative enrichment of niobium over tantalum in the late phases of crystallization of alkalic rocks. A relative enrichment of niobium over tantalum in the late-forming rocks was not observed at the Lovozero complex, but the complex does not contain basic or ultrabasic rocks, nor does it contain carbonatites. It is composed almost entirely of intermediate alkalic rocks and, therefore, would not be expected to show a pronounced enrichment in niobium in the later intrusives.

If it is assumed that successive intrusions of alkali igneous complexes are the result of fractional crystallization of an undersaturated olivine basalt as proposed by Kennedy, Barth, Erickson and Blade, and others, then the enrichment of niobium over tantalum in the late differentiates is opposite of the behavior of these two elements in saturated magmas. According to the data of Vinogradov and Rankama and Sahama (1950) there is a considerable decrease in the Nb/Ta ratio in going from basalts to andesites to granitic rocks, the normal differentiation trend of silica-rich magmas.

As additional evidence of a relative tantalum enrichment in silica-rich rocks, Rankama and Sahama (1950) list the average Nb/Ta ratio of granites as 4.8, Vinogradov lists it as 5.8, and DeKun lists it as 7. The Nb/Ta ratios of granite

pegmatites, however, is listed as 1 by DeKun and according to Solodov (1958, 1959) ranges between 0.3 and 3.0. Solodov, also reported that within a granitic pegmatite the late-forming zones have substantially lower Nb/Ta ratios than the early-forming zones, again indicating a late enrichment of tantalum.

Conclusions

In view of the proceeding discussion on the niobium and tantalum content of alkali igneous and associated rocks the following conclusions are reached.

1. The ratio of niobium to tantalum in the alkali igneous complexes as a whole is essentially the same as the ratio in the earth's crust. This is indicated by comparing the Nb/Ta ratios of the Magnet Cove, Wet Mountains, and Lovozero complexes with the average ratio of igneous rocks reported by Rankama and Sahama (1950).

2. In general, both niobium and tantalum are enriched in the alkali igneous rocks studied. Rankama (1944, 1947) gives the average niobium content of igneous rocks as 34 ppm. Nb_2O_5 and the average tantalum content as 2.5 ppm. Ta_2O_5. The data in Table XVI show that the average niobium and tantalum content of the alkali igneous rocks types is, with few exceptions, higher than the average crustal content. Gerasimovskii et. al. found a similar enrichment of both niobium and tantalum in the rocks of the Lovozero complex.

3. The niobium associated with carbonatites was in a very mobile state. This is evidenced by the enrichment of niobium in rocks intruded by carbonatites. All samples collected near carbonatites show an anomalous enrichment in niobium. These include the carbonate breccia from the Monte Largo area (ML-3), the gabbro (W-9) and replaced granite (W-3c, W-11) from the Wet Mountains, the soda syenite, (IH-16) and the Precambrian granite (IH-13) from the Iron Hill area. Other samples suspected of being enriched in niobium are the pyroxenite from the Wet Mountains (W-7) and most of the silicate rock samples from the Iron Hill area. It is believed that the niobium enters the contact rock in a metasomatic, possibly hydrothermal state and that the fluids represent the residual liquids associated with the crystallization of a volatile-rich carbonate magma. The appreciable enrichment of niobium in rocks 100 to 150 feet from a carbonatite dike suggests the possibility of locating hidden carbonatite bodies by means of geochemical prospecting.

4. There is an increasing enrichment of niobium over tantalum in the late-forming rocks of the complexes that were studied. This feature is in sharp contrast to the reported ratios from silica-rich rocks.

5. During the formation of alkali igneous complexes both niobium and tantalum enter the structure of titanium bearing minerals. The geochemical affinity of niobium and tantalum

for titanium, and to a lesser degree, zirconium has been shown by Rankama (1948), Ginzburg (1956), Fleisher et. al. (1959) and many others. Apparently, during the early stages of crystallization of alkali igneous rocks tantalum and niobium are removed in approximately equal proportions. This is indicated by the low Nb/Ta ratio of the basic and ultrabasic rocks listed in Table XVI. With continuing crystallization niobium, on the other hand, shows a stronger tendency to remain in solution and, as a result, it is concentrated in the late differentiates of the complexes. The different behavior of these two chemically similar elements is probably related to the volatile composition and content of the alkali magmas, but the exact role that volatiles play in the geochemistry of niobium and tantalum is not understood.

APPENDIX I

Brief Petrographic Description of the Analyzed Rock Samples

MC-1, nepheline syenite: a medium-grained rock consisting of orthoclase (53%), nepheline (25%), and zoned pyroxene (9%). The pyroxenes have an inner core of colorless diopside-hedenbergite rimmed by green aegirine-diopside. Accessory minerals include hornblende, sphene, apatite, magnetite, and pyrite.

MC-112, garnet nepheline syenite: a coarse-grained variety of a garnet-pseudoleucite syenite. The two rock units together comprise 24.5% of the exposed complex. The garnet-nepheline syenite consists of nepheline (15-25%), sodic orthoclase (40-60%), and pyroxenes (15%) including diopside-hedenbergite, aegirine-augite, and aegirine. The accessory minerals are a black titanium garnet, perovskite, and magnetite.

MC-173, jacupirangite: a fine-to medium-grained rock composed of more than 50% salite. Magnetite-ilmenite is abundant comprising between 2 and 25% of the rock. Apatite, biotite, sphene, garnet, and perovskite are present in amounts that sometime exceed 10%.

MC-227, trachyte: an alkalic trachyte containing sodic orthoclase (55%) and albite (30%). Accessory minerals include magnetite, sphene, apatite, pyrite, and hornblende. Small veinlets of calcite, diopside, and brown garnet cut the trachyte.

MC-216, biotite-garnet ijolite and L-17, garnet ijolite: the ijolites are distinguished primarily on the basis of the relative abundance of biotite. They contain the following minerals in widely varying amounts: nepheline, titanium garnet, diopsidic pyroxene, and biotite. The accessory minerals are apatite, pyrrhotite, perovskite, sphene, and primary calcite.

L-304, carbonatite: a medium-to coarse-grained rock composed of calcite with scattered zones enriched in apatite, brown monticellite, magnetite, black perovskite, green biotite, pyrite, and kimzeyite. The carbonatite weathers to a porous rock, mapped as "Phosphate Rock" in Figure 12, which is composed of residual minerals from the carbonatite in a matrix of secondary apatite.

ML-3, 4, 8, carbonatite: a dark grey aphanitic rock containing subhedral to euhedral fluor-apatite, subhedral to euhedral titanium-bearing magnetite, 1M or 3T phlogopite, and traces of pyrite. Calcite and more commonly dolomite form an interlocking matrix. The phlogopite often shows alteration to chamosite. Reddish brown spessartite garnet was observed in a heavy mineral fraction of the carbonatite. A brown limonitic material is scattered throughout the rock. The carbonatite contains altered and replaced inclusions, presumably fragments from the surrounding breccia. Some of the fragments contain relatively fresh alkali feldspars, but the other minerals are altered to chlorite and limonite or replaced by carbonate, apatite, and magnetite.

ML-6, carbonate breccia: composed of Precambrian rock and mineral fragments of varying size cemented by calcite and, to a lesser degree, by dolomite. Quartz, muscovite, and alkali feldspars are relatively unaltered, but may be locally replaced by carbonate. Plagioclase and ferromagnesium minerals are highly altered to sericite or chlorite and replaced by carbonate. Subhedral magnetite is abundant.

ML-12, melteigite: a fine-grained rock consisting of diopside or augitic diopside and a prismatic mineral having properties similar to those of wollastonite. Nepheline occurs as an interstitial mineral. Accessory minerals are magnetite, sphene, and apatite. Chlorite and a reddish-brown material are present as alteration products.

W-18a, 18b, pyroxenite: both are medium-grained rocks containing augite (90%), locally altered to hornblende. Minor alteration to chlorite was also observed. Magnetite is present (5%) and is often surrounded by rims of brown hornblende. Plagioclase, altered to sericite and at least as calcic rich as bytownite, occurs as an interstitial mineral.

W-7, hornblende pyroxenite: a hornblende pyroxenite composed of subhedral augite (80%), brown hornblende (10%), plagioclase (5%), and a pale green aegirine-augite (2%). Accessory minerals include biotite, magnetite and calcite. The aegirine-augite is replaced and surrounded by rims of hornblende. Also, subhedral hornblende occurs in the rock.

The plagioclase, anorthite, is often altered to sericite and replaced by calcite. Calcite also replaces the aegirine-augite.

W-16, gabbro: a medium-grained rock consisting of ophitic anorthite (70%) and augite (25%). Olivine and magnetite comprise most of the remaining rock. Aegirine-augite rims surround many of the augite grains. Brown hornblende surrounds the pyroxenes and magnetite grains.

W-10, gabbro: a medium-grained rock composed of bytownite (70%) and diopside or augite-diopside (25%). Magnetite, commonly surrounded by biotite rims, comprises the remainder of the rock.

W-9, gabbro: a rock similar to W-10 except the mafic constituents are altered to chlorite, and the plagioclase is altered to sericite, and the sample is partially replaced by carbonate.

W-12, 15, biotite-hornblende syenites: both are very coarse-grained samples composed of orthoclase (80%), green and brown hornblende (10%) and biotite (5%). Accessory minerals include perthite, magnetite, and apatite. The feldspars are partially altered to kaolinite and sericite. Hornblende and biotite are often intergrown, the biotite appearing to replace the hornblende. W-12 contains accessory hematite in addition to magnetite.

W-14, hornblende ijolite: a medium-grained rock composed of subhedral nepheline (70%) subhedral to euhedral aegirine-augite (15%) and subhedral to euhedral green hornblende (10%). Accessory minerals in order of relative abundance, are sphene, apatite, biotite, and magnetite.

W-13, biotite-hornblende-nepheline syenite: a medium- to very coarse-grained rock composed of orthoclase and perthite (60%), biotite (15%) dark green subhedral hornblende (15%), and aegirine (5%). Nepheline occurs as an interstitial accessory mineral and is often altered. Other accessory minerals include primary calcite, apatite, sphene, and magnetite.

W-8, carbonatite: a coarse-grained dike sample containing more than 90% dolomite and calcite. Fibrous, green actinolite-tremolite (5%) occurs in small clusters. A brown limonitic material fills the space between carbonate grains. In addition, a few grains of quartz were observed in the thin section.

W-17, carbonatite: a coarse-grained sample consisting of dolomite (80%) and limonite (15%). The limonite occurs as an interstitial mineral and as pseudomorphs after magnetite. Radial growths of secondary quartz surround many of the limonite pseudomorphs. Accessory minerals include apatite and muscovite.

W-3a, crocidolite carbonatite: a coarse-grained sample containing dolomite (80%) and crocidolite (15%). Fibrous crocidolite occurs as interstitial veinlets between dolomite grains and locally embays the carbonate. Hematite and limonite are also present as well as accessory apatite.

W-3b, fenite: a graphic granite in which quartz has been replaced by crocidolite. The fenite consists of orthoclase, albite and perthite (80%) that show alteration to sericite. Fibrous, often radiating growths of crocidolite (35%) embay the feldspar. Inclusions of quartz and islands of feldspar occur in the crocidolite. Carbonate, present in accessory amounts, is also embayed by crocidolite. Other accessory minerals are muscovite and magnetite.

W-3c, Precambrian granite: a coarse-grained sample partially replaced by calcite and dolomite (45%). Orthoclase, microcline, and albite sometimes zoned and commonly altered to sericite comprise 50% of the rock. The carbonate embays the feldspars and contains small embayed inclusions of quartz. Quartz is present only in accessory amounts indicating a selective replacement of quartz by carbonate. Accessory crocidolite and small euhedral grains of hematite are also present.

W-11, replaced granite: a sample of the graphic granite that has been almost completely replaced by calcite (90%) and to a lesser degree dolomite and ankerite. Remenants of orthoclase embayed and containing patches of carbonate.

IH-3, uncompahgrite: a partially altered sample containing melilite (50%) and dark brown garnet (25%). The garnet contains inclusions of melilite, magnetite (2%) and perovskite (2%). Thin perovskite rims surround many of the garnet grains and line a few fractures. Also present is a pale green pleochroic mica called phlogopite by Larsen. Some of the pyroxene and mica grains have been replaced by chlorite. Fine-grained birefringent zones of alteration border many of the fractures in the sample. Additional minerals include accessory apatite, secondary calcite, and a few primary grains of calcite.

IH-10, melteigite: a medium-to coarse-grained rock composed of pale green to clear augite (80%), nepheline (5%), anhedral sphene (5%) and subhedral apatite (5%). The nepheline occurs as late veinlets and interstitial grains often altered to a fine-grained highly birefringent material. Carbonate (4%) also occurs as interstitial grains. Biotite, present in accessory amounts, appears to replace pyroxene. Accessory perovskite and magnetite are also present in the sample.

IH-9, altered pyroxenite: a coarse-grained, gneissic-textured rock consisting of augite (70%) and biotite (25%), both altered to chlorite. Interstitial perthite is present (5%) as well as accessory sphene, apatite, and magnetite.

IH-4, ijolite: a coarse-grained variety that consists of green augite (75%) and unaltered nepheline (24%) classifying the sample as melteigite. Interstitial brown garnet appears locally to replace the pyroxene. Accessory minerals are biotite, apatite, perovskite, and an ore mineral.

IH-5, garnet melteigite: a coarse-grained rock consisting of nepheline (40%) which is altered to a fine-grained highly birefringent material, brown subhedral to euhedral garnet (30%) which is often zoned, and green prismatic crystals of aegirine-augite (25%). The garnet locally replaces the pyroxene. Accessory minerals include apatite, biotite, and magnetite.

IH-26, soda syenite: a medium-grained rock consisting of perthite (80%) and vein-like zones of green aegirine-augite (15%). Apatite (2%) and tremolite (3%) are associated with the pyroxene zones.

IH-27, nepheline syenite: a coarse-grained rock consisting of the long twinned columns of perthite and orthoclase (80%). Subhedral to euhedral hexagonal prisms of nepheline comprise approximately 10% of the sample. Biotite (5%) is the most abundant mafic constituent. Dark green aegirine (2%), euhderal sphene (1%), and accessory magnetite make up the remainder of the rock.

IH-13, Precambrian granite: a coarse-grained rock containing euhedral to subhedral orthoclase, albite, microcline, and perthite (55%). The feldspars are commonly altered to sericite. Quartz is abundant (40%) and accessory biotite is present. The sample is cut by irregular veinlets of a dark

green, fine-grained, prismatic mineral believed to be actinolite.

IH-1, carbonatite: a medium-grained rock composed of dolomite (95%), subhedral apatite (2%), and small cubes and octahedrons believed to be perovskite (1%) accessory hematite, pyrite, and chalcopyrite are present. Limonite occurs as thin irregular veinlets and as pseudomorphs after pyrite. Also, irregular veinlets of an almost opaque, yellow-brown, fibrous mineral occur in the sample.

IH-20, carbonatite: two medium-grained samples of carbonatite were collected at locality IH-20. The first consists of dolomite (95%) and phlogopite (3%). The remainder of the rock is perovskite and accessory magnetite. The second or dark sample, contains dolomite (60%), biotite surrounded by broad rims of phlogopite (30%), and brown, translucent perovskite (5%). Minute, yellow-brown needles believed to be amphibole occur in irregular veins and pierce the carbonate. Apatite (2%) and accessory hematite and magnetite are also present.

IH-30, carbonatite: a medium-grained rock composed of calcite and dolomite (50%), biotite surrounded by broad phlogopite rims (45%), and long euhedral prisms of riebeckite (2%). Magnetite, hematite, pyrite, chalcopyrite, and apatite are present in accessory amounts.

G-18, trachyte: a porphyritic rock composed almost entirely of altered feldspar (99%). Large subhedral to euhedral phenocrysts are altered to sericite and kaolinite.

Examination of fresher samples collected nearby shows the phenocrysts to be zoned, containing an albite or perthite interior and an orthoclase border. The matrix of the fresh sample consists of fine interlocking orthoclase grains. Quartz occurs in the matrix of both samples in accessory amounts. Other accessory minerals include magnetite, hematite, apatite, and rutile. Limonite occurs as pseudomorphs after magnetite and locally stains the rock.

G-33, trachyte: a porphyritic rock containing subhedral to euhedral phenocrysts of zoned orthoclase, perthite, and albite all altered to kaolinite and sericite. The matrix consists of fine-grained orthoclase and, to a lesser degree, albite and perthite. Feldspars account for 95% of the rock which is actually an albite trachyte. The remainder consists of magnetite, hematite, limonite, ilmenite, rutile, and apatite.

G-20, andesite dike: a medium-grained rock consisting of andesine (70%) which occurs as small zoned phenocrysts and as minute laths in the matrix. The feldspar is altered to kaolinite and sericite. Green hornblende (25%) is the major mafic constituent. Calcite (2%) locally replaces the andesine. Apatite, magnetite, and biotite are present in accessory amounts.

G-14, fluorite-barite rock: a medium-to coarse-grained porphyritic rock containing pink barite (25%), calcite (3%), and accessory bastnaesite, quartz, and limonite pseudomorphs after pyrite, all in a matrix of dark purple fluorite (70%).

G-26, Fluorite rock: a fine-grained sample composed almost entirely of blue and white fluorite and containing a small number of limonite pseudomorphs.

MP-1, carbonatite: a porphyritic rock containing large barite phenocrysts (60%) in a matrix, of calcite (35%). Small amounts of bastnaesite, crocidolite, and chlorite are also present.

APPENDIX II

Composition and Classification of Minerals Cited in the Text*

Mineral	Composition	Classification
Actinolite	$Ca_2(Mg,Fe)_5(OH)_2(Si_4O_{11})_2$	Amphibole
Aegirine	$NaFe(SiO_3)_2$	Pyroxene
Albite	$NaAlSi_3O_8$	Plagioclase
Oligoclase	↓	Feldspars
Andesine		↓
Labradorite		
Bytownite		
Anorthite	$CaAl_2Si_2O_8$	
Anatase	TiO_2	Oxide
Apatite	$Ca_4(CaF)(PO_4)_3$	Phosphate
Augite	$CaMgSi_2O_6$	Pyroxene
Barite	$BaSO_4$	Sulfate
Bastnaesite	$(R.E.)FCO_3$	Carbonate
Biotite	$H_2K(Mg,Fe)_3Al(SiO_4)_3$	Mica
Calcite	$CaCO_3$	Carbonate
Chalcopyrite	$CuFeS_2$	Sulfide
Chamosite	$Fe_3Al_3Si_2O_{10}\cdot 3H_2O$	Chlorite
Chlorite	Fe,Mg,Al,OH-silicate	"
Crocidolite	$NaFe(SiO_3)_2$	Amphibole
Diopside	$CaMg(SiO_3)_2$	Pyroxene
Dolomite	$(Ca,Mg)(CO_3)_2$	Carbonate
Fluorite	CaF_2	Fluoride

* According to Dana (1955)

Mineral	Composition	Classification
Hedenbergite	$CaFe(SiO_3)_2$	Pyroxene
Hematite	Fe_2O_3	Oxide
Hornblende	$NaCa_2(Mg,Fe,Al)_5(OH)_2(Si,Al)_8O_{22}$	Amphibole
Ilmenite	$FeTiO_3$	Oxide
Kaolinite	$Al_4(OH)_8Si_4O_{10}$	Clay
Kimzeyite	Zr-garnet	Garnet
Limonite	$Fe_2O_3 \cdot xH_2O$	Hydroxide
Magnetite	Fe_3O_4	Oxide
Melilite	$CaMgSiO_4$	Feldspathoid
Microcline	$KAlSi_3O_8$	Feldspar
Monticellite	$CaMgSiO_4$	Olivine
Muscovite	$H_2KAl_3(SiO_4)_3$	Mica
Nepheline	$(Na,K)(Al,Si)_2O_4$	Feldspathoid
Olivine	$(Fe,Mg)_2SiO_4$	Olivine
Orthoclase	$KAlSi_3O_8$	Feldspar
Perovskite	$CaTiO_3$	Oxide
Phlogopite	$H_2KMg_3Al(SiO_4)_3$	Mica
Pyrite	FeS_2	Sulfide
Pyrochlore	$(Na,Ca)_2(Nb,Ti)_2(O,F)_7$	Oxide
Pyrrhotite	$Fe_{1-x}S$	Sulfide
Quartz	SiO_2	Silica group
Riebeckite	$NaFe(SiO_3)_2$	Amphibole
Rutile	TiO_2	Oxide

Mineral	Composition	Classification
Salite	$Ca(Mg,Fe)Si_2O_6$	Pyroxene
Sericite	$H_2KAl_3(SiO_4)_3$	Mica
Siderite	$FeCO_3$	Carbonate
Spessartite	$Mn_3Al_2(SiO_4)_3$	Garnet
Sphene	$CaTiSiO_5$	Silicate
Wollastonite	$CaSiO_3$	Pyroxenoid

APPENDIX III

Method of Standard Deviation Calculations

The standard deviations given in Table V and Table VI were calculated by using the following equations:

$$\sigma = \sqrt{\frac{\Sigma x^2}{(n - 1)}}$$

σ = standard deviation

n = number of samples analyzed

x = deviation from the mean

The standard deviations of the Nb/Ta ratios were estimated in the following manner: 1. the standard deviation from the mean tantalum content was estimated from a plot of Ta concentration versus standard deviation (the date for this graph was obtained from Table VI); 2. the standard deviation of the ratio was calculated using the formula

$$\sigma_{Nb/Ta} = \bar{X}_{Nb/Ta} - \frac{\bar{X}_{Nb}}{\bar{X}_{Ta} + \sigma_{Ta}}$$

$\bar{X}_{Nb/Ta}$ = mean Nb/Ta ratio

$\bar{X}_{Nb}$ = mean Nb content

$\bar{X}_{Ta}$ = mean Ta content

σ_{Ta} = standard deviation of the Ta analyses.

BIBLIOGRAPHY

Ahrens, L. H. and S. R. Taylor (1961) Spectrochemical Analysis, 2nd. ed., Addison-Wesley, Reading, Mass.

Atkinson, R. H., J. Steigman, and C. F. Hiskey (1952) Analytical Chemistry of Niobium and Tantalum, Anal. Chem., vol. 24, no. 3, pp. 477-488.

Bandi, W. R., E. G. Bayak, L. L. Lewis, and L. M. Melnick (1961) Anion exchange separation of Zr, Ti, Nb, Ta, W, and Mo, Anal. Chem., vol. 33, no. 9, pp. 1275-1278.

Barth, T. F. W. (1936) The crystallization process of basalt, Am. Jour. Sci., vol. 31, no. 185, pp. 321-351.

Bergstresser, K. S. (1959) Spectrographic determination of niobium in tantalum, Anal. Chem., vol. 31, no. 11, pp. 1812-1814.

Bowen, N. L. (1924) The Fen area in Telemark, Norway, Am. Jour. Sci., vol. 8, pp. 1-11.

_____ (1926) The carbonate rocks of the Fen area in Norway, Am. Jour. Sci., vol. 12, pp. 499-503.

Brogger, W. C. (1921) Die Eruptivgesteine des Kristian-iagebiestes-IV, Kristiania Vidensk. Skir. 1, Math-Naturv. Ko. 9.

Daly, R. A. (1910) Origin of alkaline rocks, Geol. Soc. Am. Bull., vol. 21, pp. 87-118.

_____ (1918) Genesis of the alkaline rocks, Jour. Geol., vol. 26, pp. 97-134.

DeKun, N. (1962) The economic geology of columbium and tantalum, Ec. Geol., vol. 57, pp. 377-404

Dinnin, J. I. (1953) Ultraviolet spectrophotometric determination of tantalum with pyrogallol, Anal. Chem., vol. 25, no. 12, pp. 1803-1807.

Erickson, R. L. and L. V. Blade (1963) Geochemistry and petrology of the alkali igneous complex at Magnet Cove, Arkansas, U. S. Geol. Sur. Prof. Paper 425.

Es'kova, E. M. (1959) Geochemistry of Nb and Ta in the nepheline syenite massifs of the Vishnevyie Mountains, Geochem., no. 2, pp. 158-170

Fleisher, M., K. J. Murata, J. D. Fletcher, and P. F. Northen (1959) Geochemical association of niobium and titanium and its geological and economic significance, U. S. Geol. Sur., Circ. 225.

Fryklund, V. C. Jr., R. S. Harner, and E. P. Kaiser (1954) Niobium and titanium at Magnet Cove and Potash Sulphur Springs, Ark., U. S. Geol. Sur., Bull. 1015-13, pp. 25-56.

Furman, N. Howell (1962) Standard Methods of Chemical Analysis, 6th ed., vol. 1, van Nostrand, New York.

Gerasimovskii, V. I., M. M. Kakhana, L. M. Rodionova, and V. A. Vankina (1959) On the geochemistry of niobium and tantalum in the Lovozero alkalic massif, Geochem., no. 7, pp. 803-812.

Grimaldi, F. S. (1960) Determination of niobium in the parts per million range, Anal. Chem., vol. 32, no. 1 pp. 119-121.

Ginsburg, A. I. (1956) Certain features of the geochemistry of tantalum and types of tantalum enrichment, Geochem., no. 3, pp. 312-325.

Griswold, G. B. (1959) Mineral deposits of Lincoln County, New Mexico, N. Mex. Bur. Mines, Bull. 67.

Hague, J. L. and L. A. Machlan (1959) Determination of Nb and Ta in titanium base alloys, Jour. Research, Nat. Bur. of Standards, vol. 62, no. 2, pp. 53-57.

Heinrich, E. W. and A. A. Levinson (1961) Carbonatic niobium-rare earth deposits Ravalli county Montana, Am. Min., vol. 46, nos. 11-12, pp. 1424-1447.

Hillebrand, W. F. and G. E. F. Lundell (1929) Applied inorganic analysis, Wiley and Sons, New York.

Holmes, A. (1932) The origin of igneous rocks, Geol. Mag., vol. 63, pp. 543-558.

Huff, Edmund A. (1964) Anion exchange study of a number of elements in nitric-hydrofluoric acid mixtures, Anal. Chem. vol. 36, no. 10, pp. 1921-1923.

Jensen, H. I. (1908) The distribution, origin, and relationships of alkaline rocks, New South Wales Proc. Linn. Soc., vol. 33, pp. 585-586.

Johannsen, A. (1938) A Descriptive Petrography of the Igneous Rocks, vol. IV, University of Chicago Press.

Kakita, Y. and H. Goto (1962) Spectrophotometric determination of tantalum in iron, steel and niobium metal, Anal. Chem. vol. 34, no. 6, pp. 618-621.

Kallmann, S., H. Oberthin and R. Liu (1962) Determination of niobium and tantalum in minerals, ores, and concentrates using ion exchange, Anal. Chem., vol. 34, no. 6, pp. 609-613.

Kelley, V. C. (1949) Geology and economics of New Mexico iron-ore deposits, University of New Mexico Pub. in Geol. 2.

Kennedy, J. H. (1961) Polarography of niobium (V) in (ethylenedinitrilo)-tetraacetic acid and citric acid media, Anal. Chem., vol. 33, no. 7, pp. 943-946.

Kennedy, W. Q. (1933) Trends of differentiations in basaltic magmas, Am. Jour. Sci., vol. 25, pp. 239-256.

Kim, C. K. and W. W. Meinke (1963) Simultaneous determination of niobium and tantalum by neutron activation using niobium-94m and tantalum-182m and rapid radiochemical separations, Anal. Chem. vol. 35, no. 13, pp. 2135-2138.

Kirby, R. and H. Freiser (1963) Polarography of niobium-EDTA complexes, Anal. Chem., vol. 35, no. 2, pp. 122-125.

Kraus, K. A. and G. E. Moore (1951) Anion exchange studies III: separation of niobium, tantalum, and protactinium, Jour. Am. Chem. Soc., vol. 73, pp. 2900-2903.

Lambert, P. W. (1961) Petrology of the Precambrian rocks of part of the Monte Largo area, New Mexico, Master's Thesis, University of New Mexico.

Larsen, E. S. (1942) Alkali rocks of Iron Hill, Gunnison county, Colorado, U. S. Geol. Sur., Prof. Paper 197-A.

Lopez de Azcona, J. M. (1960) Investigacion geoquimica de niobio y tantalo en la provincia de la Coruna, International Geol. Cong., XX, vol. III, pp. 477-486.

Luke, C. L. (1959) Photometric determination of tantalum with phenylfluorone, Anal. Chem., vol. 31, no. 5, pp. 904-906.

McDuffie, B., W. R. Bandi, and L. M. Melnick (1959) Simultaneous spectrophotometric determination of niobium and tungsten, Anal. Chem., vol. 31, no. 8, pp. 1311-1315.

Meinke, W. W. (1959) Sensitivity charts for neutron activation analysis, Anal. Chem. vol. 31, no. 5, pp. 792-795.

Meites, L. (1963) Handbook of Analytical Chemistry, McGraw-Hill, New York.

Mitchell, B. J. (1957) X-ray spectrographic determination of tantalum, columbium, iron, and titanium oxide mixtures using simple arithmetic corrections for interelement effects, in Advances in X-ray Analysis, vol. 1, Plenum Press, New York.

Motojima, Kenji, and Hashitani (1961) Spectrophotometric determination of niobium and molybdenum with 8-quinalinol in uranium-base alloys, Anal. Chem., vol 33, no. 1, pp. 480-482.

Parker, R. L. and F. A. Hildebrand (1963) Preliminary report of alkalic intrusive rocks in the northern Wet Mountains, Colorado, U. S. Geol. Survey, Prof. Paper 450-E, pp. 8-10

Paterson, M. S. (1958) The melting of calcite in the presence of water and carbon dioxide, Am. Min., vol. 43, pp. 603-606.

Pecora, W. T. (1956) Carbonatites a review, Geol Soc. Am. Bull., vol. 87, pp. 1537-1556.

Perhac, R. M. (1960) Geology and mineral deposits of the Gallinas Mountains, New Mexico, Doctor's Thesis University of Michigan.

Rankama, K. (1944) On the geochemistry of tantalum, Bull. de la Commission Geol. de Finland, no. 133.

_____ (1947) On the geochemistry of columbium, Science, vol. 196, pp. 13-14.

_____ and Th. G. Sahama (1950) Geochemistry, University of Chicago Press.

Rowe, R. B. (1958) Niobium (columbium) deposits of Canada, Geol. Sur. Canada, Ec. Geol. Ser. no. 18.

Sandell, E. B. (1959) Colorimetric Determination of Traces of Metals, vol. III, 3rd. ed., Interscience, New York.

Shand, S. J. (1945) The present status of Daly's hypothesis of the alkaline rocks, Am. Jour. Sci., vol. 243A, pp. 495-507.

Smyth, C. H. (1913) The chemical composition of the alkaline rocks and its significance as to their origin, Am. Jour. Sci., vol. 36, pp. 33-46.

_____ (1927) The genesis of alkaline rocks, Am. Philos. Soc. Proc., vol. 66, pp. 535-580.

Solodov, N. A. (1958) Distribution of rare elements in minerals of rare-metal granite pegmatites, Geochem., no. 8, pp. 932-940.

_____ (1959) Geochemistry of rare-metal granite pegmatites, Geochem., no. 7, pp. 778-792.

Strauss, C. A. and F. C. Truter (1951) The alkali complex at Spitzkip, Geol. Soc. South Africa Trans. and Proc., vol. 53, pp. 81-130.

Tilley, C. E. (1957) Problems of alkali rock genesis, Quart. Jour. Geol. Soc. of London, vol. 113, pp. 323-360.

Turner, F. J. and J. Verhoogen (1960) Igneous and Metamorphic Petrology, 2nd ed., McGraw-Hill, New York.

Van der Veen, A. H. (1963) A study of pyrochlore, Kon. Ned. Geol. Mijnbouwkundig Genootschap, Geol. Ser. 22.

Vinogradov, A. P. (1962) Average content of chemical elements in the principal types of igneous rocks of the earth's crust, Geochem., no. 7, pp. 641-664.

Von Eckermann, H. (1948) The alkaline district of Alno Island, Sveriges Geologiska Undersokning, Ser. Ca., no. 36.

Wyllie, P. J. and O. F. Tuttle (1959) Melting of calcite in the presence of water, Am. Min., vol 44, pp. 453-459.

_____ (1960) The syetem CaO-CO_2H_2O and the Origin of Carbonatites, Jour. Petrology vol. 1, pp. 1-46.

This thesis is accepted on behalf of the faculty of the Institute by the following committee:

Frederick J. Kuellmer

Clay T. Smith

L. R. Hathaway

Dexter H. Reynolds

Marvin H. Wilkening

Date: October 21, 1964